

DEPARTMENT OF PHYSICS
UNIVERSITY OF JYVÄSKYLÄ
RESEARCH REPORT No. 4/2015

**BEYOND THE STANDARD MODEL VIA
EXTENDED SYMMETRIES AND DARK
MATTER**

**BY
TOMMI ALANNE**

Academic Dissertation
for the Degree of
Doctor of Philosophy

*To be presented, by permission of the
Faculty of Mathematics and Natural Sciences
of the University of Jyväskylä,
for public examination in Auditorium FYS1 of the
University of Jyväskylä on May 29, 2015
at 12 o'clock noon*



Jyväskylä, Finland
May 2015

Preface

The work presented in this thesis has been carried out at the Department of Physics, University of Jyväskylä, during the years 2012–2015. The work has been supervised by Doc. Kimmo Tuominen whom I would like to thank for all the inspiration and guidance starting already from a very early stage of my studies. I am grateful for this long journey that has brought me here.

The work that led to the third article of this thesis was initiated during my stay at the CP³-Origins centre, University of Southern Denmark, in Spring 2014. I would like to thank Prof. Francesco Sannino for the fruitful collaboration ever since, and the whole staff of CP³-Origins for the hospitality during my visits. The work presented here has been done in collaboration with many excellent physicists; in particular, I would like to thank Prof. Kimmo Kainulainen, Dr. Stefano Di Chiara, Mr. Ville Vaskonen, and Ms. Helene Gertov for enjoyable collaboration. I am grateful to Prof. Kari Enqvist and Prof. Arttu Rajantie for reviewing this manuscript, and to Prof. Thomas Rytto for promising to act as my opponent.

Beside the research, I have enjoyed teaching, and in particular participating in the updating of the teaching methods at the Department of Physics. Foremost, I am grateful to Dr. Pekka Koskinen for widening my perspectives for the teaching of physics. I am grateful to the whole Department of Physics, and especially to the office staff, for providing a friendly atmosphere where things work smoothly.

A great deal of making these years unforgettable is due to all my friends. Some of you I met already at the very first day of my studies, others have come along during the journey. All of you deserve huge thanks. Special thanks to the whole Holvi collaboration for the enjoyable working environment, conferences on the Baltic Sea, and discussions about life, the Universe and everything.

Finally, I would like to thank my family for all their love and support.

The financial support from the Finnish Cultural Foundation and its Central Finland Regional Fund, the Academy of Finland (Project No. 267842), the CP³-Origins centre, University of Southern Denmark, the Graduate School for Particle and Nuclear Physics, and the Faculty of Mathematics and Science and the Department of Physics, University of Jyväskylä, are gratefully acknowledged.

Abstract

In this thesis, we discuss ideas of how to go beyond the Standard Model (SM) of particle physics to incorporate the cosmological observations of dark matter and matter–antimatter asymmetry, and to address the theoretical problems related to the scalar sector of the SM.

Although the SM has proven to be an excellent description of the interactions of elementary particles, there is both experimental and theoretical evidence that this description cannot be complete. Most notably, the cosmological observations of dark matter (DM) and the matter–antimatter asymmetry in the universe cannot be explained within the SM.

We have studied simple singlet extensions of the SM. We found out that these DM and matter–antimatter-asymmetry problems cannot be solved simultaneously by adding only one real singlet scalar, but already a singlet sector consisting of the scalar and an additional fermionic DM candidate is sufficient. This study also lays the ground for more complex extensions. Further, we found out that already one additional scalar can help stabilising the SM vacuum.

Another hint beyond the SM is the vast hierarchy between the mass of the Higgs boson and the Planck scale, the natural cut-off of the SM. The naturalness problem associated with light elementary scalars motivates the study of a dynamical origin behind the electroweak symmetry breaking. Whereas an underlying strongly coupled sector can explain the hierarchy between the electroweak and the Planck scales dynamically, there is no simple way to give masses for the SM fermions without scalars. An alternative route is to combine the dynamical electroweak symmetry breaking and elementary scalars responsible for fermion masses. This is motivated by a possibility of high-energy completion of this class of models via e.g. supersymmetry or a non-trivial ultraviolet fixed point for the couplings. We have studied a specific model of this kind in the light of current data from the LHC run I and found the model viable.

The light SM Higgs boson might also imply a symmetry protecting the mass of the scalar. We have pursued this idea by extending the global symmetry of the SM scalar sector to $SU(4)$ and studied the spontaneous breaking of this global symmetry to $Sp(4)$. We found that with elementary scalars, the SM interactions breaking this global symmetry naturally prefer the Goldstone-boson nature of the Higgs boson. Further, there is a remaining pseudo-Goldstone boson that can act as a viable DM candidate producing the observed relic abundance while escaping the current stringent experimental bounds for DM detection.

List of publications

This thesis is based on the work summarised within the following publications:

- I T. Alanne, S. Di Chiara, and K. Tuominen, *LHC Data and Aspects of New Physics*, *JHEP* **1401** (2014) 041, [[arXiv:1303.3615](#)].
- II T. Alanne, K. Tuominen, and V. Vaskonen, *Strong phase transition, dark matter and vacuum stability from simple hidden sectors*, *Nucl.Phys.* **B889** (2014) 692–711, [[arXiv:1407.0688](#)].
- III T. Alanne, H. Gertov, F. Sannino, and K. Tuominen, *Elementary Goldstone Higgs and Dark Matter*, [arXiv:1411.6132](#), to appear in *Phys.Rev.* **D**.

The author participated in the numerical work, interpretation of the results, and writing of the articles [I,II]. The renormalization group and vacuum stability analysis of [II] were carried out solely by the author.

In [III], the author carried out all the numerical work and the derivation of the analytic results, and wrote the original draft of the article. He also participated in the interpretation of the results and writing the final version of the publication.

Contents

List of publications	i
1 Introduction	1
1.1 The Standard Model	1
1.2 The need to go beyond	2
1.2.1 Naturalness and hierarchy problems	3
1.2.2 Vacuum stability	3
1.2.3 Dark matter and matter–antimatter asymmetry	4
2 Dark matter and baryogenesis	5
2.1 Cold thermal relic	6
2.1.1 Relic density	6
2.1.2 Direct and indirect searches of DM	7
2.2 Electroweak baryogenesis	8
2.2.1 Sakharov conditions	8
2.2.2 Strong EWPT	9
2.3 Simple singlet extensions of the SM	9
2.3.1 Scalar DM	10
2.3.2 Fermion DM	11
3 Electroweak symmetry breaking	13
3.1 Weak dynamics	13
3.1.1 Supersymmetry	14
3.1.2 The stability of the vacuum	15
3.1.3 The Higgs mass	15
3.2 Strong dynamics	16
3.2.1 The Higgs mass	17
3.2.2 Low-energy effective theory	18
4 Bosonic technicolor	21
4.1 The effective low-energy theory	22
4.2 Validity in the light of LHC run I	23
4.3 Vector resonances and beyond run I	25
4.3.1 No direct Higgs coupling to composite vectors	25
4.3.2 Direct Higgs coupling to composite vectors	26

4.3.3	Beyond run I	27
5	Extended global symmetry and Goldstone dynamics	29
5.1	Composite Goldstone Higgs	30
5.2	Elementary Goldstone Higgs	31
5.2.1	Potential and tree-level vacuum	32
5.2.2	EW embedding	33
5.2.3	Fermions and explicit SU(4) breaking	34
5.2.4	Quantum vacuum and collider limits	35
5.2.5	Elementary Goldstone DM	37
6	Summary and outlook	39
	References	41

Chapter 1

Introduction

1.1 The Standard Model

The Standard Model of particle physics (SM) has been a triumph in trying to understand the interactions of elementary particles in terms of symmetries. It describes the strong and electroweak (EW) interactions and incorporates three generations of quarks and leptons. The interactions are based on the semi-simple gauge group $SU(3)_c \times SU(2)_L \times U(1)_Y$, where c stands for color, L for the left and Y for hypercharge.

The success of describing the electromagnetic interaction with $U(1)$ gauge symmetry mediated by a massless photon faced a challenge with weak interactions. In their study of the four-fermion interaction describing the β decay, Marshak and Sudarshan [1], and Feynman and Gell-Mann [2] proposed in the late 1950's that the four-fermion interaction could be, on a more fundamental level, mediated by a massive charged vector boson. However, since gauge symmetry prohibits adding direct mass terms for the gauge fields, the description of the weak interaction by a new gauge symmetry was in trouble.

A way out of this problem, now known as *the Higgs mechanism*, was realised independently by Englert and Brout, Higgs, and Guralnik, Hagen and Kibble in 1964 [3–5]: The gauge bosons could obtain masses, if the underlying gauge symmetry were *spontaneously broken*, i.e. if the vacuum state of the system were not symmetric under the full gauge group. This could be achieved e.g. by adding scalar multiplets transforming non-trivially under the gauge group.

A unified description of weak and electromagnetic interactions with an underlying gauge symmetry was then developed by Glashow, Weinberg, and Salam during 1960's [6–8]. In addition to the massive charged vector bosons, W^\pm , their model also conjectured the existence of an additional neutral vector boson, the Z . This EW sector of the SM was solidified theoretically by the proof of its renormalizability by 't Hooft and Veltman in 1972 [9], and experimentally first by the discovery of neutral currents in 1973 [10], and finally by the discovery of the W and Z bosons in 1983 in CERN [11, 12].

The EW sector of the SM is the minimal solution to the observed pattern of

symmetry breaking. In the SM, one adds two complex scalars transforming in the fundamental representation of the $SU(2)_L$ gauge group. The scalar potential respecting the EW gauge symmetry then reads

$$V_{\text{SM}} = m_M^2 H^\dagger H + \lambda (H^\dagger H)^2. \quad (1.1)$$

If the coefficient of the quadratic term is negative, i.e. $m_M^2 < 0$, the minimum of the potential is not at the zero value of the fields but at

$$H^\dagger H = -\frac{m_M^2}{2\lambda}, \quad (1.2)$$

and at zero there is a local maximum. The Higgs field thus acquires a non-zero vacuum expectation value (vev), $v_w^2 = \langle H^\dagger H \rangle$.

This non-zero vev then results in non-zero masses for the weak gauge bosons,

$$m_W^2 = \frac{1}{4}g^2 v_w^2 \quad \text{and} \quad m_Z^2 = \frac{1}{4}(g^2 + g'^2)v_w^2, \quad (1.3)$$

where g and g' are the gauge couplings associated with the $SU(2)_L$ and $U(1)_Y$ groups, respectively. From the EW observables one deduces the value of the Higgs vev, $v_w = 246$ GeV.

In addition to the weak gauge bosons, also the SM fermions can be given gauge symmetry preserving masses via the Higgs field by introducing Yukawa interaction terms between the fermions and the Higgs field,

$$\mathcal{L}_{\text{Yuk}} = -y_l^{ij} \bar{L}_L^i H e_R^j - y_u^{ij} \bar{Q}_L^i H^c u_R^j - y_d^{ij} \bar{Q}_L^i H d_R^j + \text{h.c.}, \quad (1.4)$$

where y_l , y_u and y_d are the Yukawa coupling matrices in the generation space, and thus the indices i, j run from one to three. Summation over repeated indices is always assumed if not otherwise stated. Although there is *a priori* no need for the masses of the fermions and the gauge bosons to come from the same source, the SM is a minimal description also in this sense.

1.2 The need to go beyond

The minimal parameterization of the elementary particles and their interactions of the SM is in excellent agreement with the experimental results from the collider experiments, and no conclusive direct evidence conflicting with the SM exists to date. However, there is rather extensive indirect evidence, both theoretical and experimental, that the SM cannot be a complete description of the nature, although being an excellent effective description at least up to the TeV scale. Below, we describe some of the cogent evidence that motivates the strive for a more complete theory.

1.2.1 Naturalness and hierarchy problems

The Higgs sector of the SM, despite its simplicity, is the most problematic part of the SM. According to the Wilsonian view of the renormalizability [13], the coefficient of the quadratic operator of the scalar potential, $H^\dagger H$, should be sensitive to the highest scale in the theory. If the SM is considered to be a complete description of the interactions of the elementary particles without taking gravity into account, this highest scale should be where the gravitational effects become important. This is the so-called Planck scale, $M_{\text{Planck}} = 1.22 \cdot 10^{19}$ GeV.

This, however, seems not to be the case with the SM Higgs having the observed mass of 125 GeV, about 17 orders of magnitude below the Planck scale. With the conventional knowledge of renormalization, this would imply rather unnatural fine-tuning of the model parameters. This is the so-called naturalness problem associated with light elementary scalars.

In the SM, we would, thus, expect that the mass of the Higgs boson, and inherently the scale of the electroweak symmetry breaking (EWSB), should be of the order of the Planck scale. The observed low scale of the EWSB is not necessarily problematic, though. For example the low scale of the quantum chromodynamics (QCD) can be well understood by the renormalization group (RG) evolution of the gauge coupling. This motivates to study alternative models where the EWSB is not due to elementary scalar fields, but would instead have a dynamical origin due to a new strongly interacting sector.

Another possible route would be to try to somehow make the elementary scalars more natural. An obvious solution along this line would be to impose some new symmetry that would then protect the mass of the scalar. Historically, the most popular symmetry extension has been the supersymmetry (SUSY). However, the minimal supersymmetric models seem to be disfavoured by the experiments motivating alternative symmetry-based approaches.

We will return to these issues in more detail in Chapter 3.

1.2.2 Vacuum stability

One hint beyond the SM is provided by the structure of the SM vacuum at high energies. By studying the RG evolution of the scalar quartic coupling one finds that the SM vacuum is actually only metastable: The quartic coupling becomes negative at $10^{10} - 10^{12}$ GeV [14, 15], implying that at high values of the scalar field, the potential is actually unbounded from below.¹ Thus, there is no true ground state for the theory. However, the lifetime of this false vacuum is longer than the age of the universe, thereby, in principle, allowing this alternative as well.

¹It should be noted that flat Minkowskian background is assumed here. It was pointed out recently by Herranen et al. [16] that neglecting the curvature effects during the inflation is rather questionable. In the de Sitter background, a non-minimal coupling to gravity is induced by loop corrections even though not present at the tree level in the Higgs potential, and this non-minimal coupling could alter the stability of the SM vacuum substantially.

However, the evolution of the scalar coupling is highly sensitive to the exact value of the top-quark Yukawa coupling. Also the dynamics beyond the SM could affect the evolution drastically. Therefore, the concept of the metastability of the vacuum without the knowledge of the correct extension of the SM is slightly misleading. Nevertheless, the metastability of the SM vacuum might hint towards the right extension, and more notably, the vacuum of the more complete theory should preferably be more stable than that of the SM. Vacuum stability is further discussed in Chapter 3.

1.2.3 Dark matter and matter–antimatter asymmetry

Currently, the most direct hint beyond the SM comes from cosmological observations: According to recent results by the Planck collaboration [17] confirming the earlier findings by WMAP [18], only about 4% of the energy budget of the universe can be explained with the SM. Over a quarter of the energy budget consists of cold dark matter (DM), and almost three quarters of the so-called dark energy. While the nature of the dark energy is highly speculative to date, the existence of DM implies additional matter fields interacting only very weakly with the SM fields.

Another cosmological observation in conflict with the SM is the excess of matter over antimatter in the universe. All the known cosmological objects seem to consist of matter; there seem to be no stars and galaxies built of antimatter. The start of the universe with a Big Bang suggests that at the very beginning, there were equal amounts of matter and antimatter. Then naively, during the cool-down of the universe, all the matter and antimatter should have annihilated leaving only photons. Therefore, to achieve the current status, at some point of the thermal evolution of the universe, the production of baryons over antibaryons must have been favoured.

Chapter 2

Dark matter and baryogenesis

The existence of DM was postulated already in 1930's. Most notably, Fritz Zwicky studied the velocities of galaxies in Coma Cluster and observed them to be higher than expected on the basis of luminous matter leading to conclusion that there was some unseen, i.e. *dark*, matter in the galaxies [19]. However, it took 40 years before the dark matter hypothesis took root due to the study of rotational curves of spiral galaxies by Vera Rubin in 1970 [20]. If the galaxies consisted only of the standard luminous matter, i.e. matter that interacts with light, the mass distribution of the galaxy could be calculated. Since the luminous matter is distributed around the centre of the spiral galaxy, the rotational velocity, according to the Kepler's law, should decrease as a function of the distance from the galactic centre far outside the luminous disc. What Rubin found out, and what was later confirmed by the the data from a large amount of galaxies, was that the stars in the outskirts of the galaxy seemed to rotate too fast. Furthermore, the velocity as a function of the radius appeared to be constant. This kind of behaviour could be explained by feebly interacting non-luminous matter halo surrounding the galaxy.

Another possible explanation to the discrepancy of the rotational curves and the expected Keplerian motion could be provided by modifying the Newtonian laws of motion at large distances. This hypothesis, however, is disfavoured by the observations of the so-called Bullet Cluster [21]. This is a dynamical system, where a small galaxy cluster collides, and goes through, a larger one. Studying the emitted light from this kind of system reveals that the colliding baryonic gas, left behind of the clusters after the collision, overweighs the baryonic matter in the galaxies that have gone through each other. Therefore, the gravitational centre of the system should be around the colliding gas. However, the study of gravitational lensing due to the system reveals that the gravitational centres are around the galaxies implying again that the galaxies are surrounded by non-interacting non-luminous matter.

In addition to the lack of a candidate for DM, the SM is short of mechanism generating the observed asymmetry between the amount of matter and antimatter in the universe. In principle, the SM already contains the ingredients for producing

an excess of baryons during the electroweak phase transition (EWPT). However, the observed Higgs boson turns out to be too heavy for the EW baryogenesis to work in the SM.

In the following, we outline the phenomenology of the cold DM, and discuss the possibilities to detect it in the future. Then, we review the Sakharov conditions for the EW baryogenesis, and discuss the strong EWPT. Finally, we consider the phenomenology of DM and EWPT in simple singlet extensions of the SM.

2.1 Cold thermal relic

2.1.1 Relic density

An abundance of DM consisting of weakly interacting massive particles (WIMPs) can be achieved, if the interactions between the WIMP candidates freeze-out of the thermal equilibrium before the interactions make the DM particles to annihilate. Qualitatively, this freeze-out happens as the mean free path of the particles reaches the size of the causal horizon.

The number density of the WIMPs can be calculated from the Lee–Weinberg equation [22]

$$\frac{\partial f(x)}{\partial x} = \frac{\langle v\sigma \rangle m^3 x^2}{H} (f^2(x) - f_{\text{eq}}^2(x)), \quad (2.1)$$

written in terms of variables $f(x) = n(x)/s_E$ and $x = s_E^{1/3}/m$. Here s_E is the entropy density at temperature T , m is the mass of the WIMP, and H is the Hubble parameter. The thermally averaged cross section can be obtained by evaluating the integral expression [23]

$$\langle v\sigma \rangle = \frac{1}{8m^4 T K_2^2(m/T)} \int_{4m^2}^{\infty} ds \sqrt{s} (s - 4m^2) K_1(\sqrt{s}/T) \sigma_{\text{tot}}(s), \quad (2.2)$$

where $K_i(y)$ are the modified Bessel functions of the second kind.

The freeze-out temperature is then fixed by studying when the number density departs from the value in the thermal equilibrium. With the knowledge of the freeze-out temperature, one can calculate the present ratio $f(0)$ of the frozen-out DM candidate. The DM abundance can be expressed by the fractional density parameter¹

$$\Omega_{\text{DM}} = \frac{\rho_{\text{DM}}(0)}{\rho_c} = \frac{s_E(0)}{\rho_c} m f(0) \approx 4.01 \cdot 10^8 m f(0), \quad (2.3)$$

and the critical density, ρ_c , can be expressed in terms of the Hubble parameter and the Newton's gravitational constant, G , as

$$\rho_c = \frac{3H^2}{8\pi G}. \quad (2.4)$$

¹Note that the number in Eq. (2.8) of [II] is incorrect. The numerical analysis was carried out with the correct value, though.

2.1.2 Direct and indirect searches of DM

There are prestigious experiments trying to observe signals from the conjectured DM particles. These experiments are typically divided into two categories, direct and indirect, depending on whether one tries to observe the DM particles scattering directly on atomic nuclei or is aiming to single out signals from DM annihilations, respectively.

Currently, the most stringent limits from the direct measurements come from the LUX experiment [24], improving the XENON100 results [25]. Both of these experiments are based on trying to detect the DM particles scattering on xenon nuclei.

There is rather heavy investment in improving the sensitivity of the direct searches. The LUX experiment still continues collecting data during 2015 with expected factor of five improvement in sensitivity. Furthermore, the on-going upgrade of the XENON100 to XENON1T is expected to improve the sensitivity of XENON100 results by about a factor of hundred. Exciting results are, therefore, expected in the near future.

In this thesis, we consider models, where the DM candidate interacts with the SM fermions only via the scalar sector. To compare the model predictions for the scattering cross section measured by LUX and XENON100, we parameterize the Higgs–nucleon coupling as $f_N m_N / v_w$, where $m_N = 0.946$ GeV is the nucleon mass (with small differences between protons and neutrons neglected) and the effective coupling between the Higgs and the nucleon,

$$f_N := \frac{1}{m_N} \sum_q \langle N | m_q \bar{q}q | N \rangle, \quad (2.5)$$

describes the normalised total quark–scalar current within the nucleon. This effective coupling is presently rather well known, and we use $f_N = 0.345 \pm 0.016$ [26]. The spin-independent scattering cross section can then be calculated from a t -channel exchange of the scalars with the nucleons in the limit $t \rightarrow 0$.

For generality, we do not want to restrict ourselves to cases where the DM abundance consists solely of one component. To allow this possibility of subdominant DM, we define f_{rel} to be the fraction of the total observed amount DM abundance,

$$f_{\text{rel}} = \Omega_{\text{DM}} h^2 / (\Omega h^2)_c, \quad (2.6)$$

where the current value of DM abundance, measured by the Planck collaboration, is $(\Omega h^2)_c = 0.12$ [17], where h is the scale factor for the present day Hubble parameter

$$H_0 = 100 h \text{ km s}^{-1} \text{ Mpc}^{-1}. \quad (2.7)$$

In the case of subdominant DM component, the correct quantity to which we want to apply the constraint from the direct searches is the predicted spin-independent cross section scaled by the fraction f_{rel} , i.e.

$$\sigma_{\text{SI}}^{\text{eff}} = f_{\text{rel}} \sigma_{\text{SI}}. \quad (2.8)$$

Another class of experimental DM searches is based on trying to detect signals from the DM annihilations in cosmological objects with high DM content. These include e.g. the galactic centre and dwarf spheroidal satellite galaxies of the Milky Way. The experiments study the γ -ray spectrum from the objects and try to find out an excess in signal due to DM annihilation to photons compared to the expected background without DM.

Most notably, of experiments along this line, the Fermi-LAT satellite has studied dwarf spheroidal satellite galaxies of the Milky Way, finding no statistically significant signal thus far [27]. However, upper limits for the DM annihilation cross section to different SM channels have been obtained. The limits are somewhat model-dependent, though, and the results rest upon e.g. the way the DM couples to the SM particle, and also slightly upon the chosen DM profile in the galaxies.

Currently, the annihilation cross section to quark and τ -lepton channels for DM particles with mass below 100 GeV, assuming the Navarro–Frenk–White DM profile of the galaxies [28], has been set to $\langle\sigma v\rangle < 2.2 \cdot 10^{-26} \text{ cm}^3 \text{ s}^{-1}$ excluding the vanilla model scenarios of thermal WIMPs in this mass range [27].

2.2 Electroweak baryogenesis

2.2.1 Sakharov conditions

In 1967, Sakharov formulated three necessary conditions for a mechanism to produce an excess of baryons over antibaryons [29]:

1. Interactions out of thermal equilibrium
2. Violation of baryon number, B .
3. Violation of C and CP .

Out-of-equilibrium interactions are needed to prevent the sphaleron wash-out of the produced baryon excess, and C and CP violation are required for the reactions to happen in the direction of producing an excess of baryons instead of erasing the possible excess. In the SM, the baryon number violation is provided via the axial anomaly of $SU(2)_L$, and consequently the Chern–Simons current [30]. The Cabibbo–Kobayashi–Maskawa mixing [31, 32] of the SM quarks entails a source of CP violation, but this is too weak to produce the observed baryon asymmetry [33, 34]. Moreover, to achieve the necessary non-equilibrium interactions, the EWPT should be strongly first order. In the SM, the EWPT is known to be continuous [35, 36]. Thus, in the SM, the obtained excess of baryons due to C , CP , and B violation is washed out by the sphaleron interactions.

2.2.2 Strong EWPT

In order to avoid the sphaleron wash-out of the generated baryon excess, the EWPT should be strongly first order. More precisely, the vev at the critical temperature in the broken phase should be comparable to the critical temperature,

$$\frac{v(T_c)}{T_c} \gtrsim 1. \quad (2.9)$$

If the SM were fully perturbative, the thermal effects would induce a cubic term in the one-loop effective scalar potential implying a first-order EWPT. However, non-perturbative effects taken into account, this picture gets altered. It was found by Kajantie et al. [35, 36] that the phase transition in the SM is of first order only if the Higgs mass is small, and for masses over 72 GeV the transition becomes a smooth crossover. Therefore, the SM with a 125 GeV Higgs does not feature a strong EWPT.

In models with multiple scalars, already the tree-level potential can incorporate multiple minima, and the transition between these minima could account for the strongly first-order EWPT. The thermal evolution of these minima can be studied taking into account only the leading thermal corrections to the mass parameters of the scalars. Studying the nature of the EWPT is thus a simple way to obtain essential knowledge of the possibility of EW baryogenesis.

2.3 Simple singlet extensions of the SM

In [II], we study simple extensions of the SM, and discuss different features of the models by studying the DM phenomenology and the nature of the EWPT. These studies illustrate the main aspects of the dichotomy between DM and baryogenesis, and therefore also lay the ground for the study of more complex extensions.²

We study two benchmark models, first with scalar DM candidate and second with fermionic DM. In both extensions, we extend the SM scalar sector by a real singlet scalar, S , described by the potential

$$V(H, S) = \mu_H^2 H^\dagger H + \lambda_H (H^\dagger H)^2 + \frac{1}{2} \mu_S^2 S^2 + \frac{\mu_3}{3} S^3 + \frac{\lambda_S}{4} S^4 + \mu_{HS} (H^\dagger H) S + \frac{\lambda_{HS}}{2} (H^\dagger H) S^2. \quad (2.10)$$

In the former case we impose a Z_2 symmetry on the potential to render the scalar DM candidate stable, i.e. set $\mu_{HS} = \mu_3 = 0$. In the latter case, we relax this symmetry requirement and add one Dirac fermion that couples to the singlet scalar. This new fermion then acts as a DM candidate.

²For a viable EW baryogenesis scenario, an additional source for CP violation is needed. In the simple singlet extensions this can be achieved e.g. by introducing a dimension-6 operator coupling the singlet scalar to the top quark [37].

In the following subsections, we outline the main aspects of these singlet extensions. Extra scalars could also play an important role in stabilising the SM vacuum. This aspect is discussed in more detail in Chapter 3.

2.3.1 Scalar DM

With only one real singlet scalar, a solution to only either DM or baryogenesis puzzles can be obtained. The explanation to this dichotomy is rather clear qualitatively: The successful DM phenomenology requires that the annihilation cross section of the DM particles is not too large in order not to annihilate all the DM before the thermal freeze out. The strong EWPT requires a rather large scalar self-interaction. Thus, in the simplest models only either of these can be achieved since both aspects are controlled effectively by a single parameter. This is clearly shown in Fig. 2.1, where we have scanned the available parameter space of the model satisfying both theoretical and experimental consistency constraints. The colour coding shows the produced fraction of the total observed amount of DM, whereas only for the points above the solid black line, the mass parameter μ_S^2 is negative allowing for multiple vacua at the tree level, thereby being the minimum requirement for the strong EWPT.³

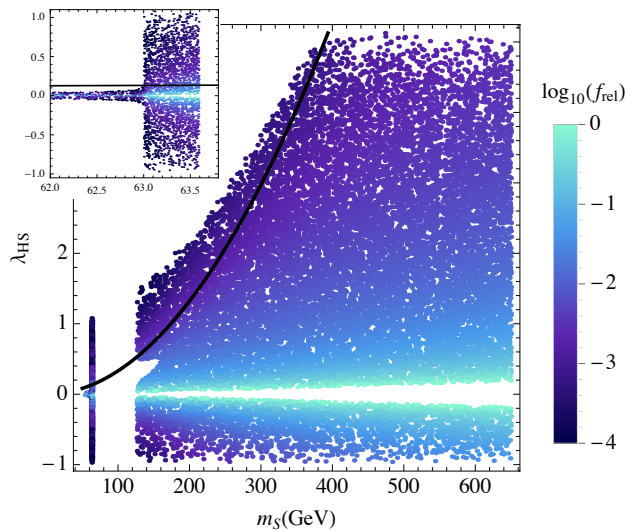


Figure 2.1: The colour coding shows the value of f_{rel} in the (m_S, λ_{HS}) plane. Above the solid black line $\mu_S^2 < 0$, and modification to the EWPT are possible. The figure is taken from [II].

³We aim for a strong EWPT at the tree level. It might be possible to get strong transition over a wider range in the parameter space from the one-loop potential, but we have not studied that possibility here.

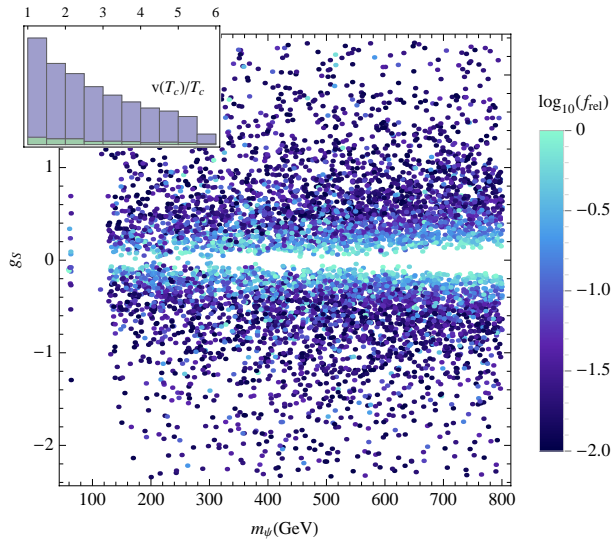


Figure 2.2: Dark matter density as a function of the dark matter mass m_ψ and the Yukawa coupling g_S . The inset shows the distribution of values of $v(T_c)/T_c$ corresponding to the points in the plot. The shaded lower portion of the histogram bars correspond to points which yield $f_{\text{rel}} > 0.5$. We show only the points which give $0.01 < f_{\text{rel}} \leq 1$, $v(T_c)/T_c > 1$ and $T_c > 40$ GeV. All shown points are also compatible with the LUX constraints. The figure is taken from [II].

2.3.2 Fermion DM

To be able to have fermionic DM, we extend the singlet sector with one Dirac fermion, ψ . The interactions of this SM-singlet fermion are given by the Lagrangian

$$\mathcal{L}_\psi = \bar{\psi} (i\cancel{\partial} - m) \psi + g_S S \bar{\psi} \psi. \quad (2.11)$$

We assume that this singlet fermion does not mix with the SM neutrinos.

If the DM is fermionic, the DM–strong-EWPT dichotomy is relaxed. Moreover, since we do not expect the singlet scalar to be a DM candidate, we do not impose the Z_2 symmetry on the scalar potential, and consequently we allow for a non-zero vev for the singlet scalar at the EW minimum. This non-zero vev then in turn contributes to the mass of the fermion. For generality, we also allow the fermion to have a Lagrangian mass term, $m\bar{\psi}\psi$, the origin of which we do not specify. Fig. 2.2 shows that in this scenario, both the strong EWPT and a substantial DM component can be easily produced.

Chapter 3

Electroweak symmetry breaking

After the detection of the massive mediators of the weak interactions and also the Higgs boson, we can, in retrospect, conclude that the gauge symmetry description of the fundamental interactions accompanied by the Higgs mechanism has proven to be a success story. However, whereas there is little doubt that the spontaneous symmetry breaking be responsible of the masses of the weak gauge bosons, there is a plethora of alternatives about what is really driving the symmetry breaking.

The general features of spontaneous symmetry breaking can be outlined without restricting within a specific model, e.g. the SM. The key point is that if the minimum of the scalar potential is not at zero value of the fields, the resulting true vacuum state then preserves less symmetries than the underlying Lagrangian describing the theory. Each of the broken generators of the symmetry group are then associated with a massless scalar mode, the so-called Goldstone boson (GB). If the underlying symmetry is a local one, the massless Goldstone modes become the longitudinal degrees of freedom of the gauge fields corresponding to the spontaneously broken generators. This is usually referred to as the massless gauge bosons eating the would-be GB's, thereby becoming massive. The scalars in question need not be elementary fields but can also be composite objects instead.

In the following, a categorisation into weak and strong dynamics is made depending on whether the dynamics behind the EWSB can be accessed by means of perturbation theory or not. We outline the benefits and shortcomings, and describe some popular scenarios related to both types of underlying dynamics.

3.1 Weak dynamics

We start by discussing the perturbative solutions behind the EWSB. The original idea behind the Higgs mechanism is to add scalar(s) transforming non-trivially under the gauge group. If the scalar self-interactions are weak, the theory is accessible via perturbation theory. One of the salient features of this approach is that it is (in principle) fully calculable, and definite predictions based on perturbation theory can be made. Moreover, the simplicity of the model with the

possibility of simultaneously incorporating fermion masses increases its appeal. However, the naturalness problem plaguing the scalars remains a troubling feature along with the possible problems with the RG evolution of the coupling constants, namely vacuum stability [14, 15], and triviality and Landau pole problems [38, 39].

A possible cure for the naturalness problem is to enlarge the Poincaré symmetry to include symmetry between fermions and bosons, i.e. supersymmetry. Although bringing forth appealing features, it suffers from one major problem: no experimental sign hinting towards near EW scale SUSY has been found implying that nature may have chosen a different path after all.

In the following, we briefly review the main features of supersymmetry before discussing other features related to weak dynamics.

3.1.1 Supersymmetry

In the early 70's, a way to include natural fundamental scalars was discovered by Golfand and Likhtman [40], and Wess and Zumino [41]. The solution was to extend the Poincaré algebra to a superalgebra (mathematically a graded algebra) by including anticommuting symmetry generators. The uniqueness of SUSY should be emphasised: The discovery of SUSY was preceded by the work of Coleman and Mandula [42] proving in 1967 that the most general symmetry group of the S -matrix is locally isomorphic to a direct product of the Poincaré and an internal symmetry group, and in 1975 Haag, Łopuszański, and Sohnius [43] showed that the direct product of SUSY and an internal symmetry group is the largest possible symmetry of the S -matrix described by graded algebras. To date, SUSY is thus the only known extension of the Poincaré symmetry.

The reason for solving the naturalness problem is that in SUSY the scalars and their fermion partners lie in the same chiral supermultiplets of the symmetry group, and consequently, the scalars inherit the chiral symmetry protection for the mass operator from the fermions. None of the predicted superpartners of the SM fields have been observed thus far, though. This can only be if the SUSY is broken at a scale above the current reach of experiments. This apparent gap between the scale of EWSB and SUSY breaking yields the so-called little hierarchy problem. Moreover, in the minimal supersymmetric extensions of the SM (MSSM), the tree-level prediction of the Higgs mass is below the Z mass [44]. Rather high level of fine-tuning is needed to push the Higgs mass up to 125 GeV by radiative corrections from the SUSY-breaking sectors. Thus, at least the minimal SUSY models seem to be reproducing the main problems they were supposed to cure. Furthermore, due to the SUSY breaking sector, the number of parameters in the minimal supersymmetric extension of the SM increases from the 19 of the SM to over a hundred.

Although near EW scale SUSY seems, in the light of the current experimental data, rather disfavoured, this does not necessarily imply the death of higher-scale SUSY. Albeit not solving the problems associated with the EWSB, high-scale SUSY would still entail many desirable features from at least partially naturalising

the scalars and possible gauge coupling unification to maybe playing a key role in unified description of SM interactions and gravity.

3.1.2 The stability of the vacuum

One of the problems of the SM is related to the quantum corrections of the scalar potential. Based on the current measurements of the top quark mass, the Yukawa interaction with the top quark seems to drive the Higgs self-coupling negative at energies $\sim 10^{10} - 10^{12}$ GeV [14, 15]. This suggests that at large values of the fields the potential is unbounded from below. This in turn would imply, were the SM the full truth up to gravitational effects, that the SM vacuum is actually a metastable one.

Additional scalars could, however, compensate the negative contribution from the top quark to the evolution of scalar self-coupling. In [II], we studied the vacuum stability in the the singlet extensions of the SM described in Chapter 2. We showed that already one singlet scalar could stabilise the Higgs vacuum up to the Planck scale, since in the RG evolution, the portal scalar coupling comes with different sign to the Yukawa coupling of the top quark. Correspondingly, additional fermions in the singlet sector coupling to the singlet scalars via Yukawa interaction could drive the self-couplings of the singlet scalars negative, giving rise to bounds on the strength of these new Yukawa interactions. Results of this analysis are shown in Fig. 3.1.

3.1.3 The Higgs mass

One of the great puzzles is the observed mass of the Higgs boson. The problem is somewhat bifurcate in the weak-dynamics scenarios: On the one hand, the Higgs mass is too light to be natural without some protecting mechanism, and on the other hand, if SUSY is invoked to naturalise the elementary scalar, the Higgs appears to be too heavy.

To be more precise, assume that a model with elementary scalars is valid, and perturbative, up to the scale Λ . Then, at a much lower energy scale, μ , we can write the scalar mass parameter to the first non-trivial order in perturbation theory as

$$m^2(\mu) = m^2(\Lambda) + c(g_i)(\Lambda^2 - \mu^2), \quad (3.1)$$

where $c(g_i)$ is a function of the marginal couplings of the model. If $\Lambda \gg \mu$, we would expect $m^2(\mu) \sim \Lambda^2$, unless there are some very peculiar cancellations between the different couplings. This peculiar cancellation could be obtained if the model is supersymmetric since the scalars and their fermion partners lie in the same representations of the super-Poincaré group. However, since the minimal supersymmetric models are not particularly favoured by the experiments, there is motivation to study other symmetry-based solutions. One possibility is a pseudo-Goldstone nature of the Higgs. This scenario is further discussed in

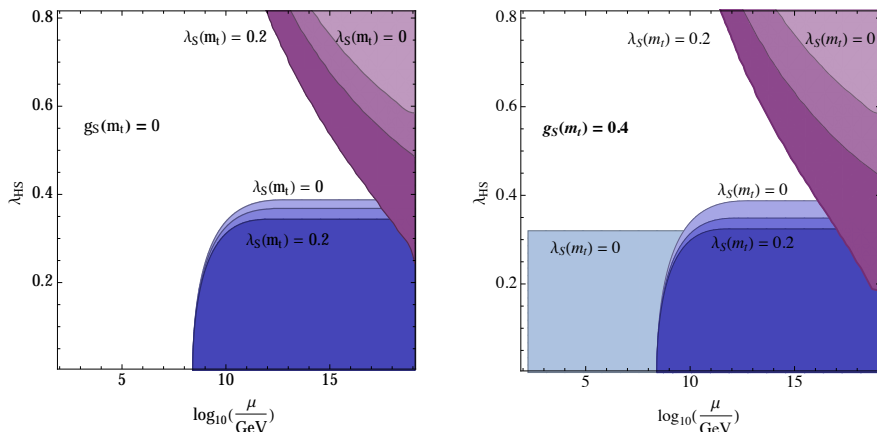


Figure 3.1: The figures show constraints from vacuum stability and perturbativity of the couplings. The contours in the lower right corner show the regions where the Higgs self-coupling becomes negative, while the contours in the upper right corner show the regions where one or more of the couplings become large. Finally, the horizontal contours correspond to the singlet self-coupling, λ_S , becoming negative. In the left panel only a real singlet scalar is included, while in the right panel the extension includes also a singlet fermion with Yukawa coupling g_S to the singlet scalar with reference value $g_S(m_t) = 0.4$. The figure in the right panel is taken from [II].

Chapter 5. The other is underlying strong dynamics behind the EWSB, and this will be discussed next.

3.2 Strong dynamics

As discussed above, the inclusion of scalars to achieve EWSB is somewhat problematic. However, even without the Higgs sector, the SM already has an EW breaking sector that does not suffer from any naturalness problems, namely the strong interaction between the quarks. By studying the RG flow of the strong coupling constant, one finds that while asymptotically free at high energies, if calculated in the perturbation theory, the coupling diverges around $\Lambda_{\text{QCD}} \sim 200$ MeV. Thus, by studying the running of a dimensionless coupling, we find an intrinsic energy scale of the theory. This is called dimensional transmutation. This energy scale, although about 20 orders of magnitude below the Planck scale, is dynamical and possesses no naturalness problems.

In reality, there is no divergence in the coupling constant, the infinity is only an artefact of the breakdown of the perturbation theory. When the coupling constant grows large enough, the quarks condense forming composite bosonic states. Since the quarks are charged under the EW gauge group, the condensate

plays the role of the Higgs boson breaking the EW symmetry spontaneously. The symmetry breaking scale of the QCD is only too low to account for the observed masses of the weak gauge bosons: the resulting masses would be over three orders of magnitude too light.

This spontaneous symmetry breaking due to underlying strong dynamics is the relativistic analogy for the time-honoured Bardeen–Cooper–Schrieffer theory of superconductivity [45–47]. At low enough temperatures, the attractive potential due to the interaction between electrons and the lattice overcomes the Coulomb repulsion resulting in the condensation of the electron pairs. These composite Cooper pairs then act as a scalar Higgs leading to spontaneous symmetry breaking and, thus, to superconductivity.

Although QCD is not quite enough to lead to the observed EWSB, it motivates to study extensions along this line. As an analogy to QCD these models were given the name technicolor (TC). The first TC models were proposed by Weinberg [48] and Susskind [49] in the late 1970’s.

Whereas the SM Higgs field gives, as a free gift, a way to generate masses for the SM fermions without breaking the gauge symmetries, this is not the case with models of dynamical symmetry breaking with strong dynamics. In order to produce the fermion masses, one needs to extend the new sector. In the absence of elementary scalars, an extended symmetry under which both the techniquarks and the SM fermions are charged should be introduced. An asset of this approach is that a dynamical explanation of the mass hierarchy of the SM fermions could (in principle) be given, while in the SM the fermion masses are only modelled, not explained. Yet, this extended technicolor (ETC) sector is the stumbling block of many TC models: if capable of producing large enough masses for the SM fermions, these ETC interactions tend to generate too large flavour-changing neutral current (FCNC) effects.

For a cure of this FCNC problem, *walking* dynamics was proposed [50]. In this scenario, the TC coupling is approximately constant, i.e. walks instead of running, between the TC and ETC scales. In order to achieve this walking behaviour in the QCD-like TC models, a large number of technifermions is needed [51], giving rise to a large contribution especially the EW S parameter [52]. Walking dynamics could be attained with fewer techniquarks, if they lie in a higher representation of the TC group. This idea was first suggested by Eichten and Lane [53], and systematised by Sannino and Tuominen [54]. This way large contributions to the S parameter could be avoided, while still featuring walking dynamics. A minimal realisation, the Minimal Walking Technicolor (MWT), contains two Dirac fermions transforming in the adjoint representation of $SU(2)_{TC}$ [54].

3.2.1 The Higgs mass

The natural mass scale of the lightest non-Goldstone state associated with the dynamical symmetry breaking would be $\sim 4\pi v_w \sim \mathcal{O}(\text{TeV})$, which is over an order of magnitude higher than the mass of the observed Higgs boson. There are

some propositions to solve this dilemma:

- **The radiative corrections due to top quark.** It was pointed out by Foadi et al. [55] that the physical mass of a composite Higgs boson does not equal to the dynamical mass due to the underlying strong dynamics because of the top quark loop corrections. Instead, the top quark induces a negative radiative mass to the composite Higgs. Therefore, to account for the observed physical mass of 125 GeV the dynamical mass of the composite should be significantly higher. It was further shown by Di Chiara et al. [56, 57] that the four-fermion interactions due to ETC sector could easily lead to an observed 125 GeV Higgs boson.
- **Techniquarks in higher representations and walking dynamics.** The mass of the lightest non-Goldstone scalar in TC models can be estimated by scaling the mass of the σ meson of QCD. If the techniquarks are in higher representations of the TC group, the resulting dynamical mass of the lightest composite scalar is reduced. Moreover, if the model features walking dynamics, the dynamical mass is expected to be further reduced. [55]
- **Goldstone boson dynamics.** Another alternative is that the observed 125 GeV scalar is a pseudo-Goldstone boson (pGB) of a larger global symmetry. In this case, the mass of the pGB Higgs is expected to be below the natural compositeness scale due to the symmetry protection. This scenario is discussed in more detail in Chapter 5.

3.2.2 Low-energy effective theory

Below the breakdown of the perturbation theory, new calculational methods must be utilised. Studying the theory on a discretized spacetime, i.e. on a spacetime lattice, has proven to give excellent results, but the limiting factor is the required computer time. Another way to estimate the features of underlying strong dynamics well below the perturbativity cut-off is to construct the low-energy effective theory adhering to the global symmetries of the underlying fundamental theory. As a first approximation, the effective theory should feature at least the lowest-spin composite states, i.e. the composite scalars. However, the characteristic feature of the fundamental strong sector is that the low-energy spectrum comprises also higher-spin resonances.

To be able to construct the corresponding effective theory, the symmetry structure of the underlying theory should be known. To this end, let us consider an $SU(N_{TC})$ gauge theory with N_f massless fermions in representation R of the gauge group. The Lagrangian can then be written in the chiral basis

$$\begin{aligned} \mathcal{L}_{\text{chiral}} &= (q_R^\dagger \ q_L^\dagger) \begin{pmatrix} 0 & i\sigma^\mu \\ i\bar{\sigma}^\mu & 0 \end{pmatrix} D_\mu \begin{pmatrix} q_L \\ q_R \end{pmatrix} \\ &= q_L^\dagger i\bar{\sigma}^\mu D_\mu q_L + q_R^\dagger i\sigma^\mu D_\mu q_R, \end{aligned} \quad (3.2)$$

where $q_{L/R}$ are the left-/right-chiral components of the fermion, and the covariant derivative reads $D_\mu = \partial_\mu - igT^a A_\mu^a$. The Lagrangian is then invariant under the chiral group $SU(N_f)_L \times SU(N_f)_R$. If the representation R is either real or pseudoreal, the global symmetry is actually $SU(2N_f)$. The larger global symmetry, $SU(2N_f)$, can be made explicit by assigning the fields q and $-i\sigma^2 q_R^*$ into one $2N_f$ component field

$$Q = \begin{pmatrix} q_L \\ -i\sigma^2 q_R^* \end{pmatrix}, \quad (3.3)$$

and then writing the chiral Lagrangian in the form

$$\mathcal{L}_{\text{chiral}} = Q^\dagger i\bar{\sigma}^\mu D_\mu Q, \quad (3.4)$$

Adding mass terms for the fermions breaks this global symmetry. The low-energy effective theory should then comply with this breaking pattern.

Characteristic for underlying strong dynamics is that it does not only predict composite scalars but also higher-spin bound states. Finding a spectrum of vector resonances would be a smoking-gun signal of new gauge symmetry with strong low-energy dynamics.

Chapter 4

Bosonic technicolor

The groundwork for extending the TC gauge group to incorporate the SM fermion masses was laid by Dimopoulos and Susskind [58], and Eichten and Lane [59]. Another route is to combine the weak and strong regimes to a model that represents dynamical EWSB due to new strong interaction, but gives masses to the SM fermions via an elementary scalar. This idea was pioneered in the late 1980's and early 1990's [60–64] and is referred here to as bosonic technicolor (bTC).

While in the general bTC framework unnaturalness of the elementary scalars is accepted, bTC-type models could be low-energy effective theories of supersymmetric technicolor models [65–67]. From the naturalness and hierarchy problem point of view this marriage of high-scale SUSY and TC-driven EWSB is very desirable: the SUSY makes the elementary scalars natural while the dynamical origin of EWSB explains the hierarchy between the SUSY-breaking and EW scales.

Another interesting route to ultraviolet (UV) completion was proposed by Litim and Sannino [68]. It was found out that if one gives up on the requirement of asymptotic freedom of the gauge coupling in gauge-Yukawa models, one could achieve a non-trivial UV fixed point for all the marginal couplings of the model leading to an *asymptotically safe* model. A very natural framework for this asymptotical safety is within the bTC models, since one requires both fermions and elementary scalars to achieve a non-trivial UV fixed point. Moreover, a fairly large amount of fermions are needed for the gauge coupling to escape the asymptotically free region. A noteworthy point is that the quadratic scalar couplings are irrelevant for the UV behaviour, thus allowing for light scalars without disturbing the asymptotical safety of the model.

In the following, we outline the main results of [I]. We concentrate on a specific bTC model called bosonic Next-to-Minimal Walking Technicolor (bNMWT) [69]. No supersymmetric nor asymptotically safe UV completion is assumed here. The effective Lagrangian is derived and studied in the light of the data from LHC run I. Moreover, the effective model is improved by taking into account the vector resonances, a characteristic feature of technicolor models, and again compared

with the collider data. Finally, prospects of the model in the light of future collider results are discussed.

4.1 The effective low-energy theory

The degrees of freedom of the low-energy theory are the elementary scalar H and the composite meson field M , describing the $SU(2)_L \times SU(2)_R$ chiral symmetry of the underlying TC theory. Both of these are transforming as doublets under the $SU(2)_L$, and the elementary and composite scalar sectors, in the absence of the interactions with fermions, are described in terms of the Lagrangians

$$\mathcal{L}_{\text{Higgs}} = D_\mu H^\dagger D^\mu H - m_H^2 H^\dagger H - \frac{\lambda_H}{3!} (H^\dagger H)^2, \quad (4.1)$$

and

$$\mathcal{L}_{\text{TC}} = D_\mu M^\dagger D^\mu M - m_M^2 M^\dagger M - \frac{\lambda_M}{3!} (M^\dagger M)^2. \quad (4.2)$$

The elementary scalar field acts as a link between the SM and the new sector via the Yukawa couplings

$$\mathcal{L}_{\text{Yuk}} = \mathcal{L}_{\text{Yuk}}^{\text{SM}} + (y_u)_{ij} H \bar{Q}_i U_j + (y_d)_{ij} \tilde{H} \bar{Q}_i D_j + (y_l)_{ij} \tilde{H} \bar{L}_i E_j + \text{h.c.}, \quad (4.3)$$

where $\mathcal{L}_{\text{Yuk}}^{\text{SM}}$ contains the SM Yukawa couplings, and $\tilde{H} = -i\sigma^2 H^*$. The Yukawa couplings with the techniquarks and the elementary Higgs generate further terms in the effective Lagrangian compared to Eq. (4.2). The full effective Lagrangian describing the technicolor sector is given by

$$\begin{aligned} \mathcal{L}_{\text{bTC}} = & D_\mu M^\dagger D^\mu M - m_M^2 M^\dagger M - \frac{\lambda_M}{3!} (M^\dagger M)^2 \\ & + \left[c_3 y_{\text{TC}} D_\mu M^\dagger D^\mu H + c_1 y_{\text{TC}} f^2 M^\dagger H + \frac{c_2 y_{\text{TC}}}{3!} (M^\dagger M) (M^\dagger H) \right. \\ & \left. + \frac{c_4 y_{\text{TC}}}{3!} \lambda_H (H^\dagger H) (M^\dagger H) + \text{h.c.} \right]. \end{aligned} \quad (4.4)$$

Notice that the Yukawa couplings of the techniquarks also induce kinetic mixing terms between the composite and elementary scalars. The EW scale, $v_w = 246$ GeV, can then be expressed in terms of the vevs of the scalars as

$$v_w^2 = v^2 + f^2 + 2c_3 y_{\text{TC}} f v, \quad \langle M \rangle = \frac{f}{\sqrt{2}}, \quad \langle H \rangle = \frac{v}{\sqrt{2}}. \quad (4.5)$$

To find out the mass eigenstates, let us start by diagonalizing the kinetic terms. The doublets H and M can be written in the kinetically diagonal basis, $M_{1,2}$, as

$$\begin{pmatrix} M \\ H \end{pmatrix} = \frac{1}{\sqrt{2}} \begin{pmatrix} A & B \\ -A & B \end{pmatrix} \begin{pmatrix} M_2 \\ M_1 \end{pmatrix}. \quad (4.6)$$

Then, we parameterize the doublets $M_{1,2}$ in terms of the charge eigenstates as

$$M_{1,2} = \begin{pmatrix} \Sigma_{1,2}^\pm \\ \frac{1}{\sqrt{2}}(f_{1,2} + \sigma_{1,2} + i\xi_{1,2}) \end{pmatrix}, \quad (4.7)$$

where $f_{1,2}$ are the vevs corresponding to the fields $M_{1,2}$, respectively.

The scalar mass eigenstates can then be obtained by rotating the charge eigenstates in (4.7):

$$\begin{aligned} \begin{pmatrix} h^0 \\ H^0 \end{pmatrix} &= \begin{pmatrix} c_\alpha & -s_\alpha \\ s_\alpha & c_\alpha \end{pmatrix} \begin{pmatrix} \sigma_2 \\ \sigma_1 \end{pmatrix}, \\ \begin{pmatrix} G^0 \\ A^0 \end{pmatrix} &= \begin{pmatrix} s_\beta & c_\beta \\ c_\beta & -s_\beta \end{pmatrix} \begin{pmatrix} \xi_2 \\ \xi_1 \end{pmatrix}, \\ \begin{pmatrix} G^\pm \\ H^\pm \end{pmatrix} &= \begin{pmatrix} s_\beta & c_\beta \\ c_\beta & -s_\beta \end{pmatrix} \begin{pmatrix} \Sigma_2^\pm \\ \Sigma_1^\pm \end{pmatrix}, \end{aligned} \quad (4.8)$$

where s_x, c_x are shorthand notations for $\sin x$ and $\cos x$. The neutral scalar h^0 is identified as the 125 GeV Higgs boson, and G^0, G^\pm are the would-be-Goldstone modes becoming the longitudinal degrees of freedom of Z and W^\pm bosons, respectively. The mixing angle β gives the ratio of the vevs, $\tan \beta = f_2/f_1$.

Since only the elementary Higgs doublet couples to the SM fermions, the FCNC's are in control [70, 71], and the low-energy effective theory corresponds to the type-I two-Higgs-doublet model (2HDM) [72]. This correspondence is shown in detail in the Appendix A of [1].

We divide the models into two distinct categories depending on the sign of the squared mass parameter of the elementary Higgs field, m_H^2 . We do this because for $m_H^2 > 0$, the SM Higgs sector cannot be responsible for the symmetry breaking, and the EWSB must be entirely due to the bTC interactions. In the following, this type of models are referred to as bTC like, whereas $m_H^2 < 0$ yields a more generic type-I 2HDM.

4.2 Validity in the light of LHC run I

To compare the underlying model with current collider data, we first parameterize the corrections to SM interactions with the following effective Lagrangian

$$\begin{aligned} \mathcal{L}_{\text{eff}} = & a_V \frac{2m_W^2}{v_w} h W_\mu^+ W^{-\mu} + a_V \frac{m_Z^2}{v_w} h Z_\mu Z^\mu - a_f \sum_{\psi=t,b,\tau} \frac{m_\psi}{v_w} h \bar{\psi} \psi \\ & + a_{V'} \frac{2m_{W'}^2}{v_w} h W_\mu'^+ W'^{-\mu} - a_S \frac{2m_S^2}{v_w} h S^+ S^-, \end{aligned} \quad (4.9)$$

where the fourth and fifth terms introduce new charged vector and scalar fields. Keeping the underlying model in mind, we scale all the couplings to SM fermions

with the same coefficient a_f . The masses are fixed to the physical masses of the particles.

We then perform a χ^2 fit for the coefficients a_i based on the results from the LHC run I and Tevatron. To compare the fit with our model, we calculate the coefficients a_i in the underlying bNMWT model. The result is

$$a_V = s_{\beta-\alpha}, \quad \text{and} \quad a_f = \frac{c_{\alpha-\rho}}{s_{\beta-\rho}} \quad (4.10)$$

for the vector and fermion coefficients, with the definitions

$$s_\rho = \sqrt{\frac{1 - c_3 y_{TC}}{2}}, \quad c_\rho = \sqrt{\frac{1 + c_3 y_{TC}}{2}}. \quad (4.11)$$

We perform a random scan over the parameter space of the model and calculate the coefficients a_V and a_f for each theoretically and experimentally viable set of parameters. The results are depicted on the (a_V, a_f) plane passing through the SM point $a_S = a_{V'} = 0$ in Fig. 4.1 with the 68%, 90%, and 95% C.L. regions based on the χ^2 fit. We see that a majority of the points lie inside the 1- σ region, although the bNMWT points are in general disfavoured compared to the SM. This is due to the fact that in bNMWT the vector coupling is always smaller than in the SM, while the LHC data favours an enhanced vector coupling.

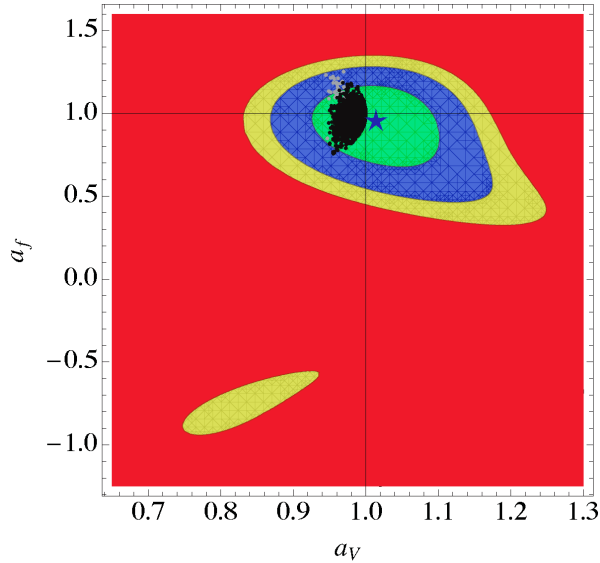


Figure 4.1: Viable data points in the (a_V, a_f) plane, together with the 68% (green), 90% (blue), and 95% (yellow) CL region: in black are the values relevant for bNMWT while those in grey refer generically to Type-I 2HDM. The blue star marks the optimal coupling coefficients on the (a_V, a_f) plane for $a_S = a_{V'} = 0$. Figure is taken from Ref. [I]

4.3 Vector resonances and beyond run I

Although the effective Lagrangian describing the fundamental and composite scalars corresponds to that of a generic type-I 2HDM, the underlying strong sector comes with rather rich low-energy spectrum. In addition to the composite scalars, also higher-spin composite states should be present in the effective description.

To correctly correspond to the underlying fundamental theory, we should include vector resonances in the effective theory in a way that preserves the gauge symmetry at the fundamental level. To this end, the principle of hidden local symmetry is used. This approach was pioneered by Bando et al. [73, 74] and was used in the framework of NMWT by Belyaev et al. [75], and earlier for MWT by Foadi et al. [76].

We outline the main steps of including vector bosons while respecting the underlying gauge invariance in [I]. The elementary gauge field, \tilde{W}^μ , couples to the composite vector bosons, and the resulting physical spectrum prior to the EWSB includes in addition to the electroweak gauge bosons, W^μ and B^μ , the vector (V^μ) and axial (A^μ) triplets. Their interactions in the vacuum respect the custodial symmetry, thereby implying no new contributions to the EW S and T parameters.

After the EWSB, the mass matrix of the charged vector fields can be written in the $(\tilde{W}^\mu, V^\mu, A^\mu)$ basis as

$$\begin{pmatrix} m_{\tilde{W}}^2 & -\frac{\epsilon m_V^2}{\sqrt{2}} & -\frac{\epsilon m_A^2}{\sqrt{2}} \\ -\frac{\epsilon m_V^2}{\sqrt{2}} & m_V^2 & 0 \\ -\frac{\epsilon m_V^2}{\sqrt{2}} & 0 & m_A^2 \end{pmatrix}, \quad (4.12)$$

where ϵ is the ratio of the weak and TC gauge couplings,

$$\epsilon := \frac{g}{g_{\text{TC}}}. \quad (4.13)$$

In the following, we consider two benchmark cases: First, we assume that only the elementary gauge field couples to the Higgs boson, and the only effect of the composite vectors is via the mixing with the elementary gauge field. Second, we allow also direct couplings between the Higgs and the composite vector resonances. To simplify the analysis, we consider the case where, in addition to the elementary gauge field \tilde{W}^μ , only the vector resonance V^μ couples to the neutral scalars. In both cases, we compare the implications of the underlying model with the fit on the LHC data.

4.3.1 No direct Higgs coupling to composite vectors

Let us consider first the case where there is no direct coupling between the Higgs and the composite vectors. In this limit, $m_V^2 = m_A^2$ and the mass of the

elementary gauge field can be written in terms of the Higgs vev and m_A as

$$m_{\tilde{W}}^2 = \frac{1}{4}g^2v_w^2 + \epsilon^2m_A^2. \quad (4.14)$$

The rotation into the mass eigenbasis is parameterized with an angle φ as

$$\begin{pmatrix} \tilde{W} \\ V \\ A \end{pmatrix} = \begin{pmatrix} c_\varphi & -s_\varphi & 0 \\ \frac{s_\varphi}{\sqrt{2}} & \frac{c_\varphi}{\sqrt{2}} & -\frac{1}{\sqrt{2}} \\ \frac{s_\varphi}{\sqrt{2}} & \frac{c_\varphi}{\sqrt{2}} & \frac{1}{\sqrt{2}} \end{pmatrix} \begin{pmatrix} W \\ W' \\ W'' \end{pmatrix}. \quad (4.15)$$

This shows that W'' does not contribute to the gauge field \tilde{W} .

We can then deduce the coefficient a_V and $a_{V'}$ parameterizing the effective Lagrangian (4.9)

$$a_V = c_{\varphi'}^2 s_{\beta-\alpha}, \quad a_{V'} = s_{\varphi'}^2 s_{\beta-\alpha}, \quad (4.16)$$

where

$$c_{\varphi'}^2 = \frac{g^2v_w^2}{4m_{\tilde{W}}^2}c_\varphi. \quad (4.17)$$

This shows that due to the mixing, the coefficient a_V is suppressed when compared to the case with only composite scalars, Eq. (4.10), and therefore we do not expect any improvement with the LHC fit. However, we find that in the region of the parameter space that is relevant to bNMWT, in particular $m_A \sim \mathcal{O}(\text{TeV})$, the modifications to the case with only scalars are small.

4.3.2 Direct Higgs coupling to composite vectors

Let us then move on to the case with also direct couplings between the Higgs and the vector resonances. The relevant terms then read [I]

$$\mathcal{L}_{hVV} \sim \frac{2m_A^2}{v_w} s_{\beta-\alpha} \left[(x^2 + \zeta s^2 \epsilon^2) \tilde{W}\tilde{W} + 2\zeta s^2 VV - 2\sqrt{2}\zeta s^2 \epsilon \tilde{W}V \right] h^0, \quad (4.18)$$

where

$$x := \frac{g_L v_w}{2m_A}, \quad (4.19)$$

s parameterizes the direct scalar-vector coupling, and ζ accounts to the rotation to the scalar mass eigenbasis,

$$\zeta := s_{\beta-\alpha}^{-1} \frac{c_{\alpha+\rho}}{s_{\beta+\rho}}. \quad (4.20)$$

The angles are defined in Eqs. (4.8) and (4.11).

The direct coupling, s , then affects the a_V and $a_{V'}$:

$$a_V = \eta_W s_{\beta-\alpha}, \quad a_{V'} = (\eta_{W'} + \eta_{W''}) s_{\beta-\alpha}, \quad (4.21)$$

and the η factors satisfy

$$\eta_W + \eta_{W'} + \eta_{W''} = 1 + \frac{2\zeta s^2}{1 + 2s^2} + \mathcal{O}(\epsilon^5). \quad (4.22)$$

The fermion and scalar coefficient remain unaltered, and a_f is given in Eq. (4.10), and a_S explicitly in Eq. (3.12) of [I].

We use the same data points as in Fig. 4.1, and calculate the coefficients a_V and $a_{V'}$ with random values of s and ϵ in the ranges $0 \leq s \leq 1$ and $0 \leq \epsilon \leq 0.1$. The results are shown in Fig. 4.2. Now the optimal point goes through a plane with non-zero $a_{V'}$, decreasing the optimal value of a_V . We thus conclude that the direct coupling to the composite vectors enables the bNMWT to reach the optimal fit to the LHC data, and additional observables are needed to further study the viability of the model.

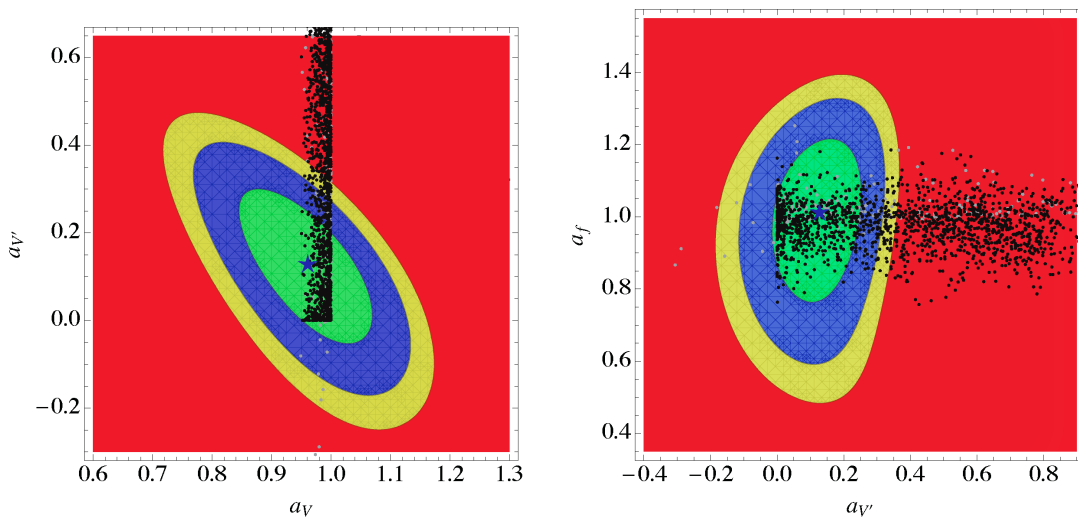


Figure 4.2: Viable data points in the $(a_V, a_{V'})$ and $(a_{V'}, a_f)$ planes, together with the 68% (green), 90% (blue), and 95% (yellow) CL region: in black are the values relevant for bNMWT ($m_H^2 > 0$) while those in grey refer generically to Type-I 2HDM ($m_H^2 < 0$) with the addition of two charged vector bosons. The blue stars mark the optimal coupling coefficients on the respective planes intersecting the optimal point with $a_S = 0$. Figures are taken from Ref. [I]

4.3.3 Beyond run I

Whereas nothing conclusive can be deduced based on the first round of the data collected at the LHC, future data should improve the situation. If nothing pointing towards new degrees of freedom are seen after the second run, the strong dynamics driven EWSB is in trouble.¹ On the other hand, if the underlying

¹There is also a possibility that the strong sector finely tuned to extreme walking with very large hierarchy between the scalar (dilaton) and other composite states.

dynamics behind the EWSB is indeed a new (natural) strong sector, a rich spectrum of new states should await us at the few-TeV scale.

Chapter 5

Extended global symmetry and Goldstone dynamics

The mass of the discovered Higgs boson is naively somewhat unexpected regardless whether one considers weak or strong dynamics underlying the EWSB. The fact that the current experimental data is not pointing towards low-scale SUSY might be hinting that there is some other kind of symmetry protecting the mass of the scalar, composite or elementary. To exhibit this idea, let us start by considering the SM Higgs potential. Parameterizing the SM Higgs doublet as

$$H = \frac{1}{\sqrt{2}} \begin{pmatrix} \phi_1 + i\phi_2 \\ \phi_3 + i\phi_4 \end{pmatrix}, \quad (5.1)$$

the most general renormalizable potential symmetric under the electroweak gauge group $SU(2)_L \times U(1)_Y$ can be written as

$$V = m_H^2 H^\dagger H + \lambda (H^\dagger H)^2 = \frac{1}{2} m_H^2 (\phi_1^2 + \phi_2^2 + \phi_3^2 + \phi_4^2) + \frac{\lambda}{4} (\phi_1^2 + \phi_2^2 + \phi_3^2 + \phi_4^2)^2. \quad (5.2)$$

The potential of (5.2) is, however, invariant under even a larger global symmetry, namely $SU(2)_L \times SU(2)_R$. This can be made explicit by writing

$$V = m_H^2 \text{Tr}[\varphi^\dagger \varphi] + \lambda \text{Tr}[\varphi^\dagger \varphi]^2, \quad (5.3)$$

where

$$\varphi = \frac{1}{\sqrt{2}} \begin{pmatrix} \phi_4 - i\phi_3 & \phi_1 + i\phi_2 \\ -(\phi_1 - i\phi_2) & \phi_4 + i\phi_3 \end{pmatrix} \quad (5.4)$$

transforms as $\varphi \rightarrow g_L \varphi g_R^\dagger$ under the global group $SU(2)_L \times SU(2)_R$. Upon the EWSB, this global symmetry breaks into the vectorial subgroup $SU(2)_V$. This is called the custodial symmetry. In the absence of the hypercharge breaking the custodial symmetry, the W^\pm and Z bosons form a triplet under the unbroken $SU(2)_V$ and have equal masses. This can be seen explicitly from the famous relation for the masses of the weak gauge bosons,

$$m_W^2 = \cos^2 \theta_W m_Z^2 = \frac{g^2}{g^2 + g'^2} m_Z^2. \quad (5.5)$$

The vectorial $SU(2)_V$ is not a symmetry of the full Lagrangian, but only of the scalar potential. The hypercharge and Yukawa interactions break this global symmetry, and the symmetry remains only approximate. However, due to this approximate symmetry, only small corrections at the quantum level are produced, and hence the name custodial symmetry. This is important, since the so-called ρ parameter, measuring the difference in the W and Z self-energies, is exactly unity at the tree level in the SM,

$$\rho = \frac{m_W^2}{m_Z^2 \cos^2 \theta_W} = 1, \quad (5.6)$$

and this tree-level value agrees with the experimental result within about 1% deviation [77].

To proceed along this line, assume that the sector responsible of the EWSB exhibits larger global symmetry than just the $SU(2)_L \times SU(2)_R$ of the SM such that upon the EWSB, additional GB degrees of freedom corresponding to the broken global symmetries emerge. The electroweak and SM Yukawa interactions do not preserve this enhanced global symmetry yielding masses at the quantum level for the Goldstone-like states associated with the global symmetry breaking. The GB's of the global symmetry breaking thus become pseudo-Goldstone bosons (pGB's) at the quantum level. However, one expects that the pGB's are significantly lighter than the other massive scalar states since their masses are generated only on the quantum level due to operators breaking the global symmetry of the scalar potential.

This kind of Goldstone dynamics can be achieved in both strongly and weakly coupled theories behind the EWSB. In the following, we shortly introduce the main features of a composite Goldstone-Higgs scenario, and then focus more on an explicit realisation of a model featuring an elementary pGB-like Higgs boson.

5.1 Composite Goldstone Higgs

To introduce the composite GB-Higgs scenario, let us consider confining strong dynamics underlying the EWSB such that the global chiral symmetry of the technifermions is larger than the global symmetry of the SM Higgs potential and contains that as a subgroup. A minimal realisation is based on the $SU(4)$ global symmetry breaking spontaneously to $Sp(4)$.¹ This global symmetry can be realised by two Dirac fermions transforming in the fundamental representation of the $SU(2)_{TC}$ gauge group. Lattice results [78, 79] support this particular breaking pattern $SU(4) \rightarrow Sp(4)$. The phenomenology of this model containing a GB-like Higgs has been studied in Refs. [80–83].

Among the notable features of this minimal scenario are [82]

¹The breaking pattern $SU(4) \rightarrow SO(4)$ associated with MWT [76] contains 9 GB's transforming as $(3, 3)$ of $SO(4) \sim SU(2)_L \times SU(2)_R$, and does not thus embody a GB Higgs.

- Due to the pGB dynamics, the mass of the lightest composite scalar state is significantly lower than the natural compositeness scale $4\pi v_w$.
- The generation of the EW scale is dynamical, and no unnatural elementary scalars are present. Some fine-tuning related to the breaking of the global symmetry is needed to achieve the desired GB dynamics.
- Extended dynamics are needed to give masses to SM fermions.
- A rich spectrum of different composite states is expected near the TeV scale.
- The topological Wess–Zumino–Witten terms [84–86] render the EW-singlet scalar unstable and thus not a suitable DM candidate.

It was shown [83] that this scenario is viable in the light of the current LHC data. Again, however, the underlying strong dynamics should show up in the future collider experiments as a rich spectrum of higher-spin composite states near the TeV scale. Thus, the analysis of the collider signatures of these higher resonances in different strong dynamical realisations is of key importance. Furthermore, extensions of the model to incorporate the SM fermion masses and a stable DM candidate are required.

5.2 Elementary Goldstone Higgs

Another route featuring Goldstone dynamics can be taken with elementary scalars. Similarly as with the composite case, the spontaneous breaking of the larger global symmetry can accommodate richer GB spectrum than required for the minimal EWSB. A natural question is whether we could identify one of the GB's as the observed Higgs particle. The GB nature of the Higgs would then imply the mass of the state to be considerably lower than the rest of the scalar spectrum.

With a richer scalar spectrum arises also the possibility to have a candidate for the DM. An intriguing possibility would be to simultaneously have both the Higgs and the DM candidate as pGB's associated with a breaking of a global symmetry. Contrary to the corresponding composite case, no topological Wess–Zumino–Witten terms [84–86] mediating the decay of the DM candidate to SM particles making it unstable arise in this case.

An advantage of the renormalizable model with elementary scalars featuring weak dynamics is that the model is perturbative, and thus, the quantum corrections can be evaluated in a controllable manner. This leads to reliable predictions of the vacuum and spectrum.

We want to pursue these ideas in the same minimal setting, $SU(4) \rightarrow Sp(4)$, as with the composite scenario to compare the different approaches. We thus have in total five GB's associated with the global symmetry breaking. Four of

the GB's transform as the SM Higgs doublet under the EW gauge group, and the remaining EW-singlet GB we identify as the DM candidate.

The breaking pattern $SU(4) \rightarrow Sp(4)$ can be achieved by having the scalar degrees of freedom transforming as a six-dimensional antisymmetric representation of the global $SU(4)$. These can be assembled into a matrix

$$M = \left[\frac{\sigma + i\Theta}{2} + \sqrt{2} \left(i\Pi_i + \tilde{\Pi}_i \right) X^i \right] E, \quad (5.7)$$

where E is an antisymmetric matrix, and X^i are Hermitian matrices corresponding to the broken generators of $SU(4)$ associated with the vacuum along E . The fields Π_i are then identified as the GB's of the spontaneous breaking of $SU(4)$ to $Sp(4)$.

In the following, we consider the renormalizable model based on this breaking pattern. We outline the main results of [III], reviewing the construction of the most general renormalizable potential at the one-loop level. Based on this, we determine the vacuum structure of the model, and finally consider collider limits and the DM phenomenology of the model.

5.2.1 Potential and tree-level vacuum

The most general renormalizable $SU(4)$ -symmetric potential for the scalar matrix variable M of Eq. (5.7) can be written as

$$\begin{aligned} V_M = & \frac{1}{2} m_M^2 \text{Tr}[M^\dagger M] + (c_M \text{Pf}(M) + \text{h.c.}) \\ & + \frac{\lambda}{4} \text{Tr}[M^\dagger M]^2 + \lambda_1 \text{Tr}[M^\dagger M M^\dagger M] - 2 (\lambda_2 \text{Pf}(M)^2 + \text{h.c.}) \\ & + \left(\frac{\lambda_3}{2} \text{Tr}[M^\dagger M] \text{Pf}(M) + \text{h.c.} \right), \end{aligned} \quad (5.8)$$

where the coefficients c_M, λ_2 , and λ_3 can, in principle, be complex, whereas m_M^2, λ , and λ_1 are real. For an antisymmetric matrix, M , the square of the Pfaffian of the matrix equals to the determinant, $\text{Pf}(M)^2 = \text{Det}(M)$; an exact definition of the Pfaffian is given in Appendix C of [III]. Note that without the Pfaffian terms, the potential is actually symmetric under the full $U(4)$ group instead of just $SU(4)$.

A sufficient condition for the quartic couplings to guarantee tree-level vacuum stability of the potential is

$$\lambda + \Delta_1 \lambda_1 - |\lambda_{2R}| - |\lambda_{2I}| - |\lambda_{3R}| - |\lambda_{3I}| \geq 0, \quad (5.9)$$

with

$$\Delta_1 = \begin{cases} 1, & \text{if } \lambda_1 \geq 0 \\ 2, & \text{if } \lambda_1 < 0 \end{cases}. \quad (5.10)$$

For simplicity, from now on we consider only real couplings and consequently drop the subscripts R .

The symmetry is broken spontaneously along E as the σ field acquires a vev

$$v^2 = \langle \sigma^2 \rangle = \frac{c_M - m_M^2}{\lambda + \lambda_1 - \lambda_2 - \lambda_3}. \quad (5.11)$$

Consequently, the σ, Θ and $\tilde{\Pi}$ fields acquire masses while the Π fields, being the GB's, remain massless.

5.2.2 EW embedding

We embed the full chiral subgroup $SU(2)_L \times SU(2)_R$ in $SU(4)$ by identifying the left and right generators as

$$T_L^i = \frac{1}{2} \begin{pmatrix} \sigma_i & 0 \\ 0 & 0 \end{pmatrix}, \quad \text{and} \quad T_R^i = \frac{1}{2} \begin{pmatrix} 0 & 0 \\ 0 & -\sigma_i^T \end{pmatrix}, \quad (5.12)$$

where σ_i are the Pauli matrices. The generator of the hypercharge is then identified with the third generator of the $SU(2)_R$ group, $T_Y = T_R^3$.

There are two inequivalent vacua associated with the breaking of $SU(4)$ to $Sp(4)$ that leave the EW symmetry intact

$$E_A = \begin{pmatrix} i\sigma_2 & 0 \\ 0 & i\sigma_2 \end{pmatrix}, \quad E_B = \begin{pmatrix} i\sigma_2 & 0 \\ 0 & -i\sigma_2 \end{pmatrix}. \quad (5.13)$$

We build our model here on E_B . Moreover, the vacuum that breaks the EW group to $U(1)_Q$ of electromagnetism, i.e. the Higgs-like vacuum, is given by

$$E_H = \begin{pmatrix} 0 & 1 \\ -1 & 0 \end{pmatrix}. \quad (5.14)$$

We want to study the general superposition of these EW conserving and EW breaking vacua, and we parameterize the vacuum as

$$E_\theta = \cos \theta E_B + \sin \theta E_H. \quad (5.15)$$

At this point, the vacuum angle, θ , is a free parameter interpolating between the Higgs-like vacuum at $\theta = \pi/2$ and the unbroken phase at $\theta = 0$. It is then convenient to reparameterize

$$M = \left[\frac{\sigma + i\Theta}{2} + \sqrt{2}(i\Pi_i + \tilde{\Pi}_i)X_\theta^i \right] E_\theta, \quad (5.16)$$

such that X_θ^i are the broken generators associated with the vacuum E_θ and Π_i are the corresponding GB's.

The electroweak subgroup of $SU(4)$ is gauged by introducing the covariant derivative

$$D_\mu M = \partial_\mu M - i(G_\mu M + M G_\mu^T), \quad (5.17)$$

where the gauge field is

$$G_\mu = gW_\mu^i T_L^i + g'B_\mu T_R^3. \quad (5.18)$$

As the scalar matrix acquires vev along E_θ ,

$$\langle M \rangle = \frac{v}{2} E_\theta, \quad (5.19)$$

the global $SU(4)$ symmetry breaks spontaneously to $Sp(4)$. Consequently, this leads to the breaking of the EW subgroup depending on the vacuum alignment yielding θ -dependent masses for the gauge bosons,

$$m_W^2 = \frac{1}{4}g^2 v^2 \sin^2 \theta, \quad \text{and} \quad m_Z^2 = \frac{1}{4}(g^2 + g'^2)v^2 \sin^2 \theta. \quad (5.20)$$

It is noteworthy that the EW scale, $v_w = v \sin \theta$, is now emergent, and the true scale of the spontaneous symmetry breaking, v , can be significantly higher.

5.2.3 Fermions and explicit $SU(4)$ breaking

To include the Yukawa interactions between the SM fermions and the scalars, we first identify the part of the scalar multiplet transforming as an $SU(2)_L$ doublet and define projectors, P_1 and P_2 that pick the components of the doublets. These projectors can be written as [81]

$$P_1 = \frac{1}{\sqrt{2}} \begin{pmatrix} 0 & 0 & 1 & 0 \\ 0 & 0 & 0 & 0 \\ -1 & 0 & 0 & 0 \\ 0 & 0 & 0 & 0 \end{pmatrix}, \quad P_2 = \frac{1}{\sqrt{2}} \begin{pmatrix} 0 & 0 & 0 & 0 \\ 0 & 0 & 1 & 0 \\ 0 & -1 & 0 & 0 \\ 0 & 0 & 0 & 0 \end{pmatrix}. \quad (5.21)$$

With the help of these projectors, we can then write down the Yukawa-interaction terms for the SM fermions invariant under the EW gauge group. For the quantum corrections to the potential, the top-quark contribution dominates over the other SM fermions, and we thus neglect their contribution to the one-loop scalar potential. The top-quark Yukawa term reads

$$\mathcal{L}_{\text{Yuk}} = y_t (Qt^c)_\alpha^\dagger \text{Tr}[P_\alpha M] + \text{h.c.} \quad (5.22)$$

As M acquires the vev along E_θ , the top quark acquires mass

$$m_t = \frac{y_t}{\sqrt{2}} v \sin \theta. \quad (5.23)$$

Having in mind to have the remaining GB as a DM candidate, we give it a small SU(4)-breaking mass term

$$V_{\text{br}} = \frac{1}{8} \mu_M^2 \text{Tr} [E_A M] \text{Tr} [E_A M]^*, \quad (5.24)$$

where E_A is given by (5.13), and $\mu_M \ll v$. In terms of the component fields, this mass term reads

$$V_{\text{br}} = \frac{1}{2} \mu_M^2 \left[(\Pi_5)^2 + (\tilde{\Pi}_5)^2 \right]. \quad (5.25)$$

Note that this is a minimal SU(4)-breaking term in the sense that it preserves the Z_2 symmetry within the original SU(4) yielding a stable DM candidate.

5.2.4 Quantum vacuum and collider limits

The quantum corrections to the scalar potential at the one-loop level are written as

$$\delta V(\Phi) = \frac{1}{64\pi^2} \text{Str} \left[\mathcal{M}^4(\Phi) \left(\log \frac{\mathcal{M}^2(\Phi)}{\mu_0^2} - C \right) \right] + V_{\text{GB}}, \quad (5.26)$$

where $\mathcal{M}(\Phi)$ is the tree-level mass matrix for the background value of the matrix of fields, M , that we denote by Φ . The supertrace, Str , is defined by

$$\text{Str} = \sum_{\text{scalars}} -2 \sum_{\text{fermions}} + 3 \sum_{\text{vectors}}. \quad (5.27)$$

We have $C = \frac{3}{2}$ for scalars and fermions, while $C = \frac{5}{6}$ for the gauge bosons. Here V_{GB} contains the GB contributions, and μ_0 is a reference renormalization scale. We have already added the appropriate counter terms to cancel the UV divergences using dimensional regularisation in the $\overline{\text{MS}}$ scheme.²

We trade the renormalization scale to the vev, v , by requiring that the vev of σ remains at the tree-level value. This condition can be written as

$$\left. \frac{\partial \delta V(\sigma)}{\partial \sigma} \right|_v = 0. \quad (5.28)$$

The minimisation of the potential with respect to the vacuum angle, θ , determines its value at the one-loop level:

$$\left. \frac{\partial \delta V(\sigma)}{\partial \theta} \right|_v = 0, \quad \text{and} \quad \left. \frac{\partial^2 \delta V(\sigma)}{\partial \theta^2} \right|_v > 0. \quad (5.29)$$

To reduce the number of unknowns, we fix a common tree-level mass scale for the massive scalars, i.e. we set $M_\sigma = M_\Theta = M_{\tilde{\Pi}} =: M_S$. In this limit, the free

²Treating the GB corrections to the potential as done with the massive scalars would lead to infrared divergences due to their vanishing masses. There are several ways of dealing with this issue, for example adding some characteristic mass scale as an infrared regulator. However, since the massive scalars give the dominant contribution to the vacuum structure of the theory, we simply neglect the GB contributions.

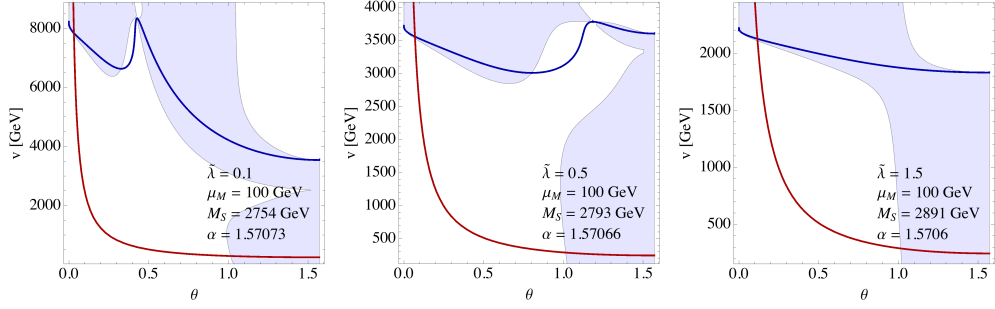


Figure 5.1: The blue contour represents the stationary points with respect to θ , the blue regions show where the second derivative with respect to θ is positive (stationary point contour on a blue region is thus a minimum) and the red contour shows the points that give the correct EW gauge boson and top-quark masses. The tree-level masses of all the heavy scalars are assumed to be of the same order, M_S , and its value is fixed by identifying lightest eigenstate of the $\sigma - \Pi_4$ mixing with the observed 125 GeV scalar. The figures are taken from Ref. [III].

parameters are M_S, v , and a combination of the quartic couplings, $\lambda + 4\lambda_1 =: \tilde{\lambda}$. Further, we fix v by requiring that the model produces the correct EW spectrum, i.e $v \sin \theta = v_w$. Taking the quantum corrections into account, the σ and Π_4 states mix. The mass eigenstates can be obtained by a rotation

$$\begin{pmatrix} \sigma \\ \Pi_4 \end{pmatrix} = \begin{pmatrix} \cos \alpha & -\sin \alpha \\ \sin \alpha & \cos \alpha \end{pmatrix} \begin{pmatrix} h^0 \\ H^0 \end{pmatrix}, \quad (5.30)$$

and the lightest eigenstate, h^0 , is identified with the 125 GeV Higgs. This fixes M_S , leaving only $\tilde{\lambda}$ and μ_M as free parameters. The value of the explicit SU(4)-breaking mass, μ_M , plays a negligible role in the analysis of the quantum vacuum, and we fix it to a benchmark value, $\mu_M = 100$ GeV.

We plot the results for different values of $\tilde{\lambda}$ in Fig. 5.1. Eminent feature here is that due to the requirement of renormalizability, the pGB nature of the Higgs is naturally preferred.

Next, we want to compare the different Higgs couplings predicted by the model with the current LHC results. The relevant couplings to compare are

$$\begin{aligned} \lambda_{hhhh} &= 6\lambda_{\text{eff}}, & \lambda_{hhh} &= 6\lambda_{\text{eff}} v \cos \alpha \\ g_{hWW} &= \frac{1}{2}g^2 v \sin \theta \sin(\theta + \alpha), & g_{hZZ} &= \frac{1}{2}(g^2 + g'^2)v \sin \theta \sin(\theta + \alpha) \\ y_{hff} &= \frac{y_f}{\sqrt{2}} \sin(\theta + \alpha), \end{aligned} \quad (5.31)$$

where $\lambda_{\text{eff}} = \lambda + \lambda_1 - \lambda_2 - \lambda_3$. The deviations from the SM results can be parameterized with the coefficients a_i , as (cf. Eq. (4.9)). The model predictions for the vector and fermion coefficients are

$$a_V = \frac{g_{hVV}}{g_{hVV}^{\text{SM}}} = \sin(\theta + \alpha), \quad \text{and} \quad a_f = \frac{y_{hff}}{y_{hff}^{\text{SM}}} = \sin(\theta + \alpha). \quad (5.32)$$

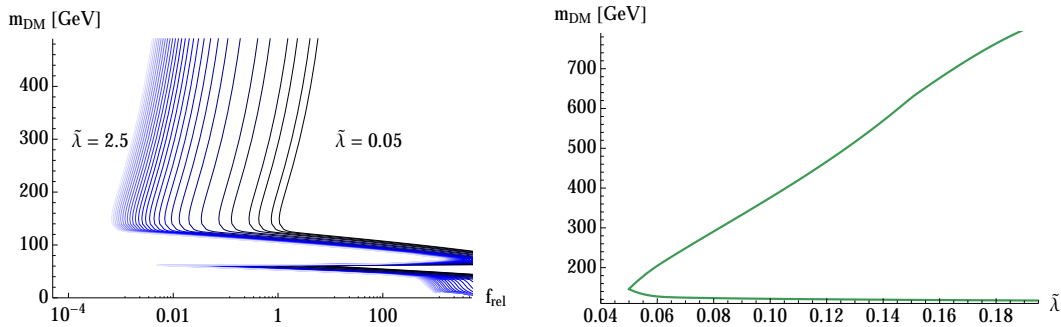


Figure 5.2: **Left panel:** The mass of the DM candidate as a function of the fraction of the total observed DM abundance, f_{rel} , for $\tilde{\lambda}$ varying from 0.05 to 2.5. The curves correspond to parameter values that fulfil the minimisation condition with respect to the vacuum angle, θ , produce the observed EW spectrum, and give the correct Higgs mass. **Right panel:** The contour giving $f_{\text{rel}} = 1$ in the $(\tilde{\lambda}, m_{\text{DM}})$ plane. The figures are taken from Ref. [III].

Since the vacuum angle θ is predicted to be very small, and the mixing angle $\alpha \sim \pi/2$, see Fig. 5.1, we expect the couplings to vector bosons and fermions to be near the SM values. Indeed, we found that only less than 3% modifications to the fermion and vector couplings are predicted even for very large $\tilde{\lambda} \leq 10$. The current bounds from the CMS experiment [87] for the modification factors are

$$a_V = 1.01_{-0.07}^{+0.07}, \quad \text{and} \quad a_f = 0.89_{-0.13}^{+0.14}. \quad (5.33)$$

The model is therefore in good agreement with the current bounds.

However, the Higgs trilinear coupling is expected to be highly suppressed compared with the SM value. In the limit of equal tree-level scalar masses, the trilinear coupling can be written as

$$\lambda_{hhh} = \frac{3M_S^2 \cos \alpha}{v}, \quad (5.34)$$

where the suppression due to the mixing angle, $\alpha \sim \pi/2$, is explicit. For $\tilde{\lambda} = 0.1$, the trilinear coupling is only 0.1% of the SM value and grows up to 3.5% for $\tilde{\lambda} = 10$. This makes the trilinear coupling an interesting probe for the future collider experiments.

5.2.5 Elementary Goldstone DM

Contrary to the composite case, the topological Wess–Zumino–Witten terms are absent due to renormalizability of the model, and the fifth pGB as a stable particle serves as a DM candidate. We can calculate its thermal relic density by using the Lee–Weinberg equation, Eq. (2.1). The small explicit SU(4) breaking

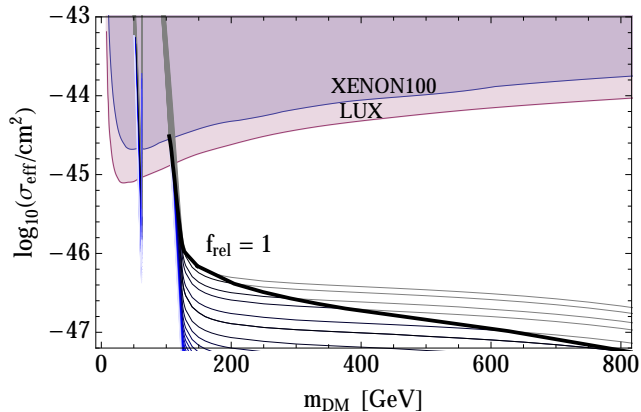


Figure 5.3: The spin-independent cross section as a function of the mass of the DM candidate for the the same cases already depicted in Fig. 5.2 with the approximate $f_{\text{rel}} = 1$ contour. The grey parts produce too large DM relic abundance and are, thus, excluded. The figure is taken from Ref. [III].

allows us to vary the mass of the DM candidate without significantly altering the vacuum structure and EW spectrum. The resulting fraction of the thermal DM relic density is depicted in the left panel of Fig. 5.2. In the right panel of Fig. 5.2, the contour giving the total observed amount of DM abundance, i.e. $f_{\text{rel}} = 1$, is shown in (λ, m_{DM}) plane.

The resulting spin-independent cross section of the DM scattering on the SM nuclei is then compared with the exclusion limits from LUX. The curves corresponding to those in Fig. 5.2 are then depicted in Fig. 5.3 with the LUX exclusion limits. The black curve indicates $f_{\text{rel}} = 1$. We conclude that in the mass range $m_{\text{DM}} \gtrsim m_h$, the model is well below the current direct-detection bounds while still producing the full observed DM relic abundance.

We further note that in this mass range, the model is consistent also with the most stringent indirect-detection bounds provided by the Fermi-LAT experiment studying the γ -ray spectrum of dwarf satellite galaxies of the Milky Way for DM annihilation signals. As discussed in Chapter 2, the Fermi-LAT collaboration has been able to exclude the thermal relic annihilation cross section, $\langle\sigma v\rangle = 2.2 \times 10^{-26} \text{ cm}^3\text{s}^{-1}$, for WIMPs up to $m_{\text{DM}} \lesssim 100 \text{ GeV}$ [27].

Chapter 6

Summary and outlook

Despite the success of the SM as a description of the interactions of the elementary particles, there is both theoretical and experimental evidence that the SM is only a good effective description valid at least up to the EW scale. The theoretical problems related to the Higgs sector along with the cosmological observations of the DM and matter–antimatter asymmetry in the universe motivate to strive towards a more complete description of the particle interactions.

In this thesis, we have presented extensions beyond the SM motivated by enhanced symmetries and the explanation of the DM. The hierarchy and naturalness problems related to the EWSB via a light elementary scalar motivate the study of models with EWSB due to a dynamical origin similar to the QCD or superconductivity. However, replacing the elementary scalars by composite fermionic states faces a problem in the generating the masses for the SM fermions. Whereas in the SM the Higgs field, needed for giving masses for the weak gauge bosons via spontaneous symmetry breaking, can also very conveniently give masses to the SM quarks and leptons, this cannot be easily attained without elementary scalars. In this case the new strong sector must be extended in rather complicated manner to achieve the observed spectrum.

As a complementary route, we have discussed bTC models, where the dynamical origin of the EWSB and the generation of the masses for the SM fermions due to elementary scalars are combined. The possibility of UV completion of this class of models via either supersymmetry or a UV fixed point for the coupling constants referred to as asymptotic safety further motivate the study along this line. In [I], we have studied the implications of the data from the first run of the LHC on a specific bTC model and found this type of models consistent with the experiments. However, if the EWSB has a strongly interacting dynamical origin, a rich spectrum of new composite states near the TeV scale should appear at the future collider experiments. A detailed study of collider imprints in different strong dynamical realisations is thus essential for the next run.

Presently, the most direct evidence beyond the SM comes from the cosmological observations of DM and matter–antimatter asymmetry in the universe. Neither of these problems can be solved without extending the SM somehow.

Conversely, these could, and should, be used as a guideline beyond the SM. To elucidate the basic features of extending the SM towards explaining the DM abundance or the genesis of an excess of baryons over antibaryons, we studied simple singlet extensions of the SM in [II]. Most notably, the observed DM abundance and the strong EWPT prefer different regions of the parameter space of the simplest extensions suggesting that these two phenomena cannot have exactly the same origin. Moreover, the study of singlet extensions showed that the addition of extra scalar degrees of freedom potentially improves the stability of the SM vacuum.

A common puzzle for either weak- or strong-dynamics origin of the EWSB is the observed light Higgs boson. This might suggest that there is some symmetry protecting the Higgs mass. Since no experimental evidence of supersymmetry exists to date, it is highly compelling to study other symmetry-based approaches. One possibility is that the observed Higgs boson is a pGB of an enhanced global symmetry. This can be realised either with composite or elementary scalars. In [III], we studied a realisation of this scenario with elementary scalars exhibiting spontaneous global symmetry breaking pattern $SU(4) \rightarrow Sp(4)$. The novel and desirable feature, when compared with the composite case, is that the quantum corrections due to the top quark along with the requirement of renormalizability automatically prefer the GB-like Higgs boson, whereas the corresponding strong-dynamics realisation prefer the TC limit without additional symmetry breaking operators. Furthermore, the remaining EW-neutral pGB of the global symmetry breaking is stable contrary to the composite case where topological terms induce the decay of the remaining pGB to SM fermions. Thus, it can act as a DM candidate and, as found out in [III], produce the observed relic abundance without conflicting the current experimental bounds. The pGB nature of the Higgs boson suggests that the trilinear Higgs self-coupling is highly suppressed when compared to the SM case, providing an interesting probe for the future collider experiments.

We know that the SM cannot be a complete description of the nature. The new physics could appear in many forms: the origin of the EWSB could be dynamical and this should show up as a rich spectrum of new composite states, or alternatively, the observed Higgs particle could be elementary and only the first elementary scalar of many to be discovered. In this thesis, we have encompassed different avenues of extending the SM that will provide further directions for future studies. Should there be new discoveries at the LHC in the future, we know that they must represent physics beyond the SM.

References

- [1] E. Sudarshan and R. Marshak, *Chirality invariance and the universal Fermi interaction*, *Phys.Rev.* **109** (1958) 1860–1860.
- [2] R. Feynman and M. Gell-Mann, *Theory of Fermi interaction*, *Phys.Rev.* **109** (1958) 193–198.
- [3] F. Englert and R. Brout, *Broken Symmetry and the Mass of Gauge Vector Mesons*, *Phys.Rev.Lett.* **13** (1964) 321–323.
- [4] P. W. Higgs, *Broken Symmetries and the Masses of Gauge Bosons*, *Phys.Rev.Lett.* **13** (1964) 508–509.
- [5] G. Guralnik, C. Hagen, and T. Kibble, *Global Conservation Laws and Massless Particles*, *Phys.Rev.Lett.* **13** (1964) 585–587.
- [6] S. Glashow, *Partial Symmetries of Weak Interactions*, *Nucl.Phys.* **22** (1961) 579–588.
- [7] S. Weinberg, *A Model of Leptons*, *Phys.Rev.Lett.* **19** (1967) 1264–1266.
- [8] A. Salam, *Weak and Electromagnetic Interactions*, *Conf.Proc.* **C680519** (1968) 367–377.
- [9] G. 't Hooft and M. Veltman, *Regularization and Renormalization of Gauge Fields*, *Nucl.Phys.* **B44** (1972) 189–213.
- [10] **Gargamelle Neutrino** Collaboration, F. Hasert et al., *Observation of Neutrino Like Interactions Without Muon Or Electron in the Gargamelle Neutrino Experiment*, *Phys.Lett.* **B46** (1973) 138–140.
- [11] **UA1** Collaboration, G. Arnison et al., *Experimental Observation of Isolated Large Transverse Energy Electrons with Associated Missing Energy at $s^{*(1/2)} = 540\text{-GeV}$* , *Phys.Lett.* **B122** (1983) 103–116.
- [12] **UA1** Collaboration, G. Arnison et al., *Experimental Observation of Lepton Pairs of Invariant Mass Around $95\text{-GeV}/c^{**2}$ at the CERN SPS Collider*, *Phys.Lett.* **B126** (1983) 398–410.

- [13] K. Wilson and J. B. Kogut, *The Renormalization group and the epsilon expansion*, *Phys.Rept.* **12** (1974) 75–200.
- [14] G. Degrandi, S. Di Vita, J. Elias-Miro, J. R. Espinosa, G. F. Giudice, et al., *Higgs mass and vacuum stability in the Standard Model at NNLO*, *JHEP* **1208** (2012) 098, [arXiv:1205.6497].
- [15] O. Antipin, M. Gillioz, J. Krog, E. Mølgaard, and F. Sannino, *Standard Model Vacuum Stability and Weyl Consistency Conditions*, *JHEP* **1308** (2013) 034, [arXiv:1306.3234].
- [16] M. Herranen, T. Markkanen, S. Nurmi, and A. Rajantie, *Spacetime curvature and the Higgs stability during inflation*, *Phys.Rev.Lett.* **113** (2014), no. 21 211102, [arXiv:1407.3141].
- [17] **Planck** Collaboration, P. Ade et al., *Planck 2013 results. XVI. Cosmological parameters*, *Astron.Astrophys.* **571** (2014) A16, [arXiv:1303.5076].
- [18] **WMAP** Collaboration, E. Komatsu et al., *Seven-Year Wilkinson Microwave Anisotropy Probe (WMAP) Observations: Cosmological Interpretation*, *Astrophys.J.Suppl.* **192** (2011) 18, [arXiv:1001.4538].
- [19] F. Zwicky, *Die Rotverschiebung von extragalaktischen Nebeln*, *Helv.Phys.Acta* **6** (1933) 110–127.
- [20] V. C. Rubin and W. Kent Ford, Jr., *Rotation of the Andromeda Nebula from a Spectroscopic Survey of Emission Regions*, *Astrophys.J.* **159** (1970) 379–403.
- [21] D. Clowe, M. Bradac, A. H. Gonzalez, M. Markevitch, S. W. Randall, et al., *A direct empirical proof of the existence of dark matter*, *Astrophys.J.* **648** (2006) L109–L113, [astro-ph/0608407].
- [22] B. W. Lee and S. Weinberg, *Cosmological Lower Bound on Heavy Neutrino Masses*, *Phys.Rev.Lett.* **39** (1977) 165–168.
- [23] P. Gondolo and G. Gelmini, *Cosmic abundances of stable particles: Improved analysis*, *Nucl.Phys.* **B360** (1991) 145–179.
- [24] **LUX** Collaboration, D. Akerib et al., *First results from the LUX dark matter experiment at the Sanford Underground Research Facility*, *Phys.Rev.Lett.* **112** (2014) 091303, [arXiv:1310.8214].
- [25] **XENON100** Collaboration, E. Aprile et al., *Dark Matter Results from 225 Live Days of XENON100 Data*, *Phys.Rev.Lett.* **109** (2012) 181301, [arXiv:1207.5988].

- [26] J. M. Cline, K. Kainulainen, P. Scott, and C. Weniger, *Update on scalar singlet dark matter*, *Phys.Rev.* **D88** (2013) 055025, [arXiv:1306.4710].
- [27] **Fermi-LAT** Collaboration, M. Ackermann et al., *Searching for Dark Matter Annihilation from Milky Way Dwarf Spheroidal Galaxies with Six Years of Fermi-LAT Data*, arXiv:1503.0264.
- [28] J. F. Navarro, C. S. Frenk, and S. D. White, *A Universal density profile from hierarchical clustering*, *Astrophys.J.* **490** (1997) 493–508, [astro-ph/9611107].
- [29] A. Sakharov, *Violation of CP Invariance, c Asymmetry, and Baryon Asymmetry of the Universe*, *Pisma Zh.Eksp.Teor.Fiz.* **5** (1967) 32–35.
- [30] S.-S. Chern and J. Simons, *Characteristic forms and geometric invariants*, *Annals Math.* **99** (1974) 48–69.
- [31] N. Cabibbo, *Unitary Symmetry and Leptonic Decays*, *Phys.Rev.Lett.* **10** (1963) 531–533.
- [32] M. Kobayashi and T. Maskawa, *CP Violation in the Renormalizable Theory of Weak Interaction*, *Prog.Theor.Phys.* **49** (1973) 652–657.
- [33] M. Shaposhnikov, *Baryon Asymmetry of the Universe in Standard Electroweak Theory*, *Nucl.Phys.* **B287** (1987) 757–775.
- [34] M. Shaposhnikov, *Structure of the High Temperature Gauge Ground State and Electroweak Production of the Baryon Asymmetry*, *Nucl.Phys.* **B299** (1988) 797.
- [35] K. Kajantie, M. Laine, K. Rummukainen, and M. E. Shaposhnikov, *Is there a hot electroweak phase transition at $m(H)$ larger or equal to $m(W)$?*, *Phys.Rev.Lett.* **77** (1996) 2887–2890, [hep-ph/9605288].
- [36] K. Rummukainen, M. Tsypin, K. Kajantie, M. Laine, and M. E. Shaposhnikov, *The Universality class of the electroweak theory*, *Nucl.Phys.* **B532** (1998) 283–314, [hep-lat/9805013].
- [37] J. M. Cline and K. Kainulainen, *Electroweak baryogenesis and dark matter from a singlet Higgs*, *JCAP* **1301** (2013) 012, [arXiv:1210.4196].
- [38] M. Lindner, *Implications of Triviality for the Standard Model*, *Z.Phys.* **C31** (1986) 295.
- [39] D. J. Callaway, *Triviality Pursuit: Can Elementary Scalar Particles Exist?*, *Phys.Rept.* **167** (1988) 241.
- [40] Y. Golfand and E. Likhtman, *Extension of the Algebra of Poincare Group Generators and Violation of p Invariance*, *JETP Lett.* **13** (1971) 323–326.

- [41] J. Wess and B. Zumino, *Supergauge Transformations in Four-Dimensions*, *Nucl.Phys.* **B70** (1974) 39–50.
- [42] S. R. Coleman and J. Mandula, *All Possible Symmetries of the S Matrix*, *Phys.Rev.* **159** (1967) 1251–1256.
- [43] R. Haag, J. T. Lopuszanski, and M. Sohnius, *All Possible Generators of Supersymmetries of the s Matrix*, *Nucl.Phys.* **B88** (1975) 257.
- [44] K. Inoue, A. Kakuto, H. Komatsu, and S. Takeshita, *Low-Energy Parameters and Particle Masses in a Supersymmetric Grand Unified Model*, *Prog.Theor.Phys.* **67** (1982) 1889.
- [45] L. N. Cooper, *Bound electron pairs in a degenerate Fermi gas*, *Phys.Rev.* **104** (1956) 1189–1190.
- [46] J. Bardeen, L. Cooper, and J. Schrieffer, *Theory of superconductivity*, *Phys.Rev.* **108** (1957) 1175–1204.
- [47] J. Bardeen, L. Cooper, and J. Schrieffer, *Microscopic theory of superconductivity*, *Phys.Rev.* **106** (1957) 162.
- [48] S. Weinberg, *Implications of Dynamical Symmetry Breaking*, *Phys.Rev.* **D13** (1976) 974–996.
- [49] L. Susskind, *Dynamics of Spontaneous Symmetry Breaking in the Weinberg-Salam Theory*, *Phys.Rev.* **D20** (1979) 2619–2625.
- [50] B. Holdom, *Raising the Sideways Scale*, *Phys.Rev.* **D24** (1981) 1441.
- [51] D. D. Dietrich and F. Sannino, *Conformal window of $SU(N)$ gauge theories with fermions in higher dimensional representations*, *Phys.Rev.* **D75** (2007) 085018, [[hep-ph/0611341](#)].
- [52] M. E. Peskin and T. Takeuchi, *Estimation of oblique electroweak corrections*, *Phys.Rev.* **D46** (1992) 381–409.
- [53] K. D. Lane and E. Eichten, *Two Scale Technicolor*, *Phys.Lett.* **B222** (1989) 274.
- [54] F. Sannino and K. Tuominen, *Orientifold theory dynamics and symmetry breaking*, *Phys.Rev.* **D71** (2005) 051901, [[hep-ph/0405209](#)].
- [55] R. Foadi, M. T. Frandsen, and F. Sannino, *125 GeV Higgs boson from a not so light technicolor scalar*, *Phys.Rev.* **D87** (2013), no. 9 095001, [[arXiv:1211.1083](#)].
- [56] S. Di Chiara, R. Foadi, and K. Tuominen, *125 GeV Higgs from a chiral techniquark model*, *Phys.Rev.* **D90** (2014), no. 11 115016, [[arXiv:1405.7154](#)].

- [57] S. Di Chiara, R. Foadi, K. Tuominen, and S. Tähtinen, *Dynamical Origin of the Electroweak Scale and the 125 GeV Scalar*, [arXiv:1412.7835](#).
- [58] S. Dimopoulos and L. Susskind, *Mass Without Scalars*, *Nucl.Phys.* **B155** (1979) 237–252.
- [59] E. Eichten and K. D. Lane, *Dynamical Breaking of Weak Interaction Symmetries*, *Phys.Lett.* **B90** (1980) 125–130.
- [60] E. H. Simmons, *Phenomenology of a Technicolor Model With Heavy Scalar Doublet*, *Nucl.Phys.* **B312** (1989) 253.
- [61] A. Kagan and S. Samuel, *Renormalization group aspects of bosonic technicolor*, *Phys.Lett.* **B270** (1991) 37–44.
- [62] C. D. Carone and E. H. Simmons, *Oblique corrections in technicolor with a scalar*, *Nucl.Phys.* **B397** (1993) 591–615, [[hep-ph/9207273](#)].
- [63] C. D. Carone and H. Georgi, *Technicolor with a massless scalar doublet*, *Phys.Rev.* **D49** (1994) 1427–1436, [[hep-ph/9308205](#)].
- [64] C. D. Carone, E. H. Simmons, and Y. Su, *$b \rightarrow s\gamma$ and $Z \rightarrow b\bar{b}$ in technicolor with scalars*, *Phys.Lett.* **B344** (1995) 287–292, [[hep-ph/9410242](#)].
- [65] M. Dine, W. Fischler, and M. Srednicki, *Supersymmetric Technicolor*, *Nucl.Phys.* **B189** (1981) 575–593.
- [66] M. Antola, S. Di Chiara, F. Sannino, and K. Tuominen, *Minimal Super Technicolor*, *Eur.Phys.J.* **C71** (2011) 1784, [[arXiv:1001.2040](#)].
- [67] M. Antola, S. Di Chiara, F. Sannino, and K. Tuominen, *Supersymmetric Extension of Technicolor & Fermion Mass Generation*, *Nucl.Phys.* **B864** (2012) 664–693, [[arXiv:1111.1009](#)].
- [68] D. F. Litim and F. Sannino, *Asymptotic safety guaranteed*, *JHEP* **1412** (2014) 178, [[arXiv:1406.2337](#)].
- [69] M. Antola, M. Heikinheimo, F. Sannino, and K. Tuominen, *Unnatural Origin of Fermion Masses for Technicolor*, *JHEP* **1003** (2010) 050, [[arXiv:0910.3681](#)].
- [70] S. L. Glashow and S. Weinberg, *Natural Conservation Laws for Neutral Currents*, *Phys.Rev.* **D15** (1977) 1958.
- [71] E. Paschos, *Diagonal Neutral Currents*, *Phys.Rev.* **D15** (1977) 1966.
- [72] G. Branco, P. Ferreira, L. Lavoura, M. Rebelo, M. Sher, et al., *Theory and phenomenology of two-Higgs-doublet models*, *Phys.Rept.* **516** (2012) 1–102, [[arXiv:1106.0034](#)].

- [73] M. Bando, T. Kugo, S. Uehara, K. Yamawaki, and T. Yanagida, *Is rho Meson a Dynamical Gauge Boson of Hidden Local Symmetry?*, *Phys.Rev.Lett.* **54** (1985) 1215.
- [74] M. Bando, T. Kugo, and K. Yamawaki, *Composite Gauge Bosons and 'Low-energy Theorems' of Hidden Local Symmetries*, *Prog.Theor.Phys.* **73** (1985) 1541.
- [75] A. Belyaev, R. Foadi, M. T. Frandsen, M. Jarvinen, F. Sannino, et al., *Technicolor Walks at the LHC*, *Phys.Rev.* **D79** (2009) 035006, [[arXiv:0809.0793](#)].
- [76] R. Foadi, M. T. Frandsen, T. A. Rytto, and F. Sannino, *Minimal Walking Technicolor: Set Up for Collider Physics*, *Phys.Rev.* **D76** (2007) 055005, [[arXiv:0706.1696](#)].
- [77] **Particle Data Group** Collaboration, K. Olive et al., *Review of Particle Physics*, *Chin.Phys.* **C38** (2014) 090001.
- [78] R. Lewis, C. Pica, and F. Sannino, *Light Asymmetric Dark Matter on the Lattice: SU(2) Technicolor with Two Fundamental Flavors*, *Phys.Rev.* **D85** (2012) 014504, [[arXiv:1109.3513](#)].
- [79] A. Hietanen, R. Lewis, C. Pica, and F. Sannino, *Composite Goldstone Dark Matter: Experimental Predictions from the Lattice*, *JHEP* **1412** (2014) 130, [[arXiv:1308.4130](#)].
- [80] E. Katz, A. E. Nelson, and D. G. Walker, *The Intermediate Higgs*, *JHEP* **0508** (2005) 074, [[hep-ph/0504252](#)].
- [81] J. Galloway, J. A. Evans, M. A. Luty, and R. A. Tacchi, *Minimal Conformal Technicolor and Precision Electroweak Tests*, *JHEP* **1010** (2010) 086, [[arXiv:1001.1361](#)].
- [82] G. Cacciapaglia and F. Sannino, *Fundamental Composite (Goldstone) Higgs Dynamics*, *JHEP* **1404** (2014) 111, [[arXiv:1402.0233](#)].
- [83] A. Arbey, G. Cacciapaglia, H. Cai, A. Deandrea, S. Le Corre, et al., *Fundamental Composite Electroweak Dynamics: Status at the LHC*, [arXiv:1502.0471](#).
- [84] J. Wess and B. Zumino, *Consequences of anomalous Ward identities*, *Phys.Lett.* **B37** (1971) 95.
- [85] E. Witten, *Nonabelian Bosonization in Two-Dimensions*, *Commun.Math.Phys.* **92** (1984) 455–472.
- [86] E. Witten, *Global Aspects of Current Algebra*, *Nucl.Phys.* **B223** (1983) 422–432.

- [87] **CMS** Collaboration, *Precise determination of the mass of the Higgs boson and studies of the compatibility of its couplings with the standard model*, *CMS-PAS-HIG-14-009* (2014).